Lowag, J., Bull, J.M., Vardy, M.E., Miller, H. and Pinson, L.J.W. (2012) High-resolution seismic imaging of a Younger Dryas and Holocene mass movement complex in glacial lake Windermere, UK. *Geomorphology*, 171-172, 42-57. (doi:10.1016/j.geomorph.2012.05.002).

High-resolution seismic imaging of a Younger Dryas and Holocene mass movement complex in glacial lake Windermere, UK

J. Lowag [*,1], J.M. Bull, M.E. Vardy, H. Miller, L.J.W. Pinson

School of Ocean and Earth Science, National Oceanography Centre Southampton, University of Southampton Water Front Campus, European Way, Southampton SO14 3ZH, UK

[1] Present address: Innomar Technologie GmbH, Schutower Ringstr. 4, 18069 Rostock, Germany

[*] Corresponding Author. E-mail address: jlowag@innomar.com, Phone: +49 381 440790, Fax: +49 381 44079299

Abstract

The stratigraphy and sedimentological processes operating over the last 15,000 years within glacial lake Windermere (UK), at the mouth of Cunsey Beck, were imaged by a decimetre-resolution seismic reflection survey. A complex of fifteen mass movement deposits were identified as contemporaneous with the Younger Dryas, and two within the overlying Holocene drape. The high vertical resolution and dense grid of profiles allowed pseudo three-dimensional mapping of individual events, along with the determination of their relative temporal relationships. The size of the mass wasting deposits has been estimated to range between 2,100 m^3 and more than 100,000 m^3. The geometry, structure and relationship to the existing stratigraphy suggests a rapid emplacement of the Younger Dryas mass movement deposits, facilitated by climatic changes making subaqueous slopes unstable, with possible triggering by seismic activity. Morphometric parameters, such as volume and planar surface area, indicates a greater mobility of the Younger Dryas mass movement deposits compared to the Holocene events. The sediments of all imaged mass movement deposits are believed to originate from the slope deposits of the lake. The age of two Holocene mass movement deposits, triggered by flooding or terrestrial debris flows, is estimated to be 2,400 and 4,400 years B.P.

Keywords: High-resolution seismic; Younger Dryas; Holocene; Mass movement; Windermere; Parametric sub-bottom profiler

1. Introduction

Lake deposits can provide a continuous, high-resolution record of sedimentation processes associated with environmental changes without the erosional unconformities usually found in sub-aerial deposits. Sediment provenance, environmental conditions, vegetation, fauna and changes due to anthropogenic influence are recorded within lacustrine sediments (Shen et al., 2008). Furthermore, catastrophic events such as seismic and volcanic activities, rockfalls, floods, extreme river discharges and mass movements, sourced onshore as well as below the lake level, leave their fingerprint in the sedimentary succession (Schnellmann et al., 2006). For glacigenic lakes the limiting boundary for tracing back these events is usually the last glaciation, during which ice related erosion removed all previous deposits.

High-resolution seismic reflection surveying is commonly used to study the large- and small-scale morphological and stratigraphic features associated with the depositional history (Scholz, 2001). For absolute dating purposes, core analysis is often combined with geophysical methods (Todd et al., 2008). Mass movements related to continental margins and in the marine realm are well studied due to their large size, their geo-hazard potential and the availability of industrial 3D seismic data sets (e.g., Hühnerbach and Masson, 2004; Haflidason et al., 2004; Masson et al., 2006). Previous studies of late glacial and Holocene sediments in lacustrine and fjord environments has focused on general stratigraphic and morphological interpretation (Mullins and Halfmann, 2001; Baster et al., 2003; Schnellmann et al., 2006; Vardy et al., 2010). Mass movement deposits have been imaged and linked to palaeoseismic events (Schnellmann et al., 2002; Waldmann et al., 2011). Depositional processes and mobility in weakly consolidated lacustrine sediments have been addressed (Schnellmann et al., 2005; Moernaut and De Batist, 2011), but are still not well understood.

Here we investigate the depositional history of late glacial and Holocene sediments in the South Basin of glacial lake Windermere, UK, and the morphological characteristics of a series of subaqueous mass movements dating back to late glacial and mid-Holocene times. Windermere has been investigated using Chirp and multi-channel boomer data in the past (Pinson, 2009;

Vardy et al., 2010) to gain an understanding of the overall history of the lake deposits from active ice-retreat at the end of the last glaciation through to modern lakebed processes. As part of this, a decimetre-resolution 3D seismic volume was acquired to investigate a locally confined mass movement complex in the North Basin of the lake (Vardy et al., 2010). In this study, we applied a parametric sub-bottom profiler to image a region in the South Basin (which is less well studied) around two mass movements visible in swath bathymetry data at high lateral detail and with decimetre vertical resolution. The study area is located close to the mouth of Cunsey Beck, the major source of sediment flux into the South Basin. The sub-bottom data revealed two events within the Holocene deposits and 15 nested events within the underlying postglacial deposits in an area of approximately 600 m x 800 m. The high-resolution of the data set allowed a reconstruction of the spatial relationship of the individual events, their individual morphology, as well as an assessment of the likely sources, timing and processes for their emplacement. This study will contribute to the available morphological database of lacustrine mass movement deposits and will also address questions related to the timing and triggering of mass movements events and their mobility.

2. Regional setting and the study area

Windermere is located in the south eastern part of the Lake District, UK, and is a North-South trending ribbon lake, separated into a North and South Basin by a bedrock high. The lake has an area of 14.8 km^2 and an overall length of about 17 km, with the North Basin being significantly wider (up to 1.5 km) than the South Basin (typically 0.5 km). The mean lake level is c. 35 m above present sea level and the maximum water depth is 62 m (northern end of the North Basin).

Our study area is located at the mouth of Cunsey Beck (Fig. 1). This river delivers the main sediment flux into the South Basin from a catchment area around Esthwaite Water to the west of the lake, with an approximate catchment size of 20.7 km^2 (Fig. 1). Esthwaite Water acts as a sediment trap for some of the coarse grained particles, but the majority of fines are transported further into the basin of Windermere. Maximum terrestrial slope angles at the lake shore are about 10° however the western lake shore around Cunsey Beck is more gently dipping (c. 5°). Where Cunsey Beck enters Windermere, the lake is 950 m wide, and has a maximum water depth of 35 m. The shore proximal parts of the lake have water depths of less than 20 m, with a major break of slope at c. 200 m from the western shore, and at greater than 300 m from the eastern shore, giving rise to steep slopes (up to 17°) dipping down into the deeper basin.

The basement rocks of the region are of Silurian age (Lawrence et al., 1986). The entire southern lake basin is underlain by banded siltstones and mudstones with subordinate sandstone turbidites of the Bannisdale Formation of the Windermere Supergroup (Millward et al., 2000). Several major synclines and anticlines with a South West – North East trend are present at both southern lake shores. A major fault, downthrowing to the west (Fig. 1), is inferred to run along the lake axis (Lawrence et al., 1986), from the outcrop of the Windermere Supergroup to the south to the outcrop of the Borrowdale Volcanic Group north of the lake.

The modern valley morphology was shaped by glaciers during the Devensian glaciations between 120 ka and 11.7 ka BP and subsequent fluvial processes. The maximum extent of the British and Irish Ice Sheet (BIIS) during the Last Glacial Maximum (LGM) was located south of Windermere (Clark et al., 2010; Chiverrell and Thomas, 2010). Optically stimulated luminescence (OSL) dating suggests ice in the Windermere area had thinned enough to expose the high peaks by 16 ka BP (16.5 ± 1.7 ka BP at New Close and 19.4 ± 2.6 ka BP at Warton Crag; Telfer et al., 2009). Furthermore, based on ^{36}Cl exposure ages, Ballantyne et al. (2009) suggest a substantial ice-loss in the SW Lake District by c. 17 ka BP, which broadly agrees with pollen records and early ^{14}C dating of organic-rich succession in lake cores (Pennington, 1943, 1977; Coope et al., 1977). Retreat of this ice mass from the Windermere valley left a complex sequence of BIIS glaciogenic landforms preserved in the lake sediments (Pinson, 2009).

This was followed by the Windermere Interstadial (more widely referred to as Bølling/Allerød interstadial), before onset of the subsequent Younger Dryas cooling and related local ice readvance. The small valley and cirque glaciers (which may have developed into plateau ice fields; McDougall, 2001) during this period, did not reach Windermere (Sissons, 1980; McDougall, 2001), therefore leaving BIIS ice retreat features and post glacial deposits excellently preserved. However, the Younger Dryas ice was within the lake catchment, and this led to a distinct change in the sedimentation regime within the lake (Pennington, 1943, 1977; Mackereth, 1971). By the onset of the Holocene at about 11.7 ka BP (NGRIP event stratigraphy and GICC05 chronology, Lowe et al., 2008) the whole region was ice-free (Pennington, 1943, 1977; Coope et al., 1977).

3. Methods

A 2D seismic reflection data set was collected in April 2011, using an Innomar™ parametric sub-bottom profiler, side-mounted onto the vessel *R/V The John Lund*. Parametric profilers have the advantage of narrow focused beams, short pulses with wide frequency bandwidth, and convenient small transducer sizes (Wunderlich et al., 2005). Parametric systems produce two slightly different primary frequencies which generate new secondary frequencies (the sum and difference of the primary frequencies), which are received and analysed. The Innomar™ system used here transmits primary frequencies around a centre frequency of 100 kHz, which generate secondary frequencies between 5 and 15 kHz. For the small transducer size used (22 x 22 cm) the half-power beam width (at -3 dB) is a very narrow 3.8˚ (Table 1).

Regional survey lines were acquired at 50 m spacing, with a more densely spaced grid of 10 m lines over two debris flows (Fig. 2) identified in swath bathymetry data. A survey speed of around 2 m s^{-1} was used, which together with a heave compensator to reduce vertical movements due to wave action, resulted in very good data quality. Positioning was by Differential GPS, and lake level data was recorded with a tide gauge. Variations of the lake level during the survey were in the range of ± 5 cm, and therefore static corrections were not applied to the seismic reflection data. A sound velocity profile was performed daily, and indicated that there was no significant layering within water column. All seismic data was band-pass filtered (6 – 18 kHz), and an envelope function was applied to aid interpretation.

The parametric seismic profiles gave a penetration of up to 20 m below the lakebed. Due to the selected dominant frequency of 12 kHz and a bandwidth of c. 10 kHz, a vertical resolution of better than 10 cm was achieved. In addition to the parametric data, a previously recorded multi-channel boomer seismic profile was used to correlate this data with the wider stratigraphic context (Pinson, 2009; Fig. 3). The boomer system, with a frequency band between 0.4 kHz and 4.0 kHz, imaged deeper and achieved a vertical resolution of about 30 cm. The ice retreat surface was imaged in the boomer data, at a depth of slightly more than 30 m below the lakebed. All parametric sub-bottom profiler sections were depth converted with a constant acoustic velocity of 1435 m s^{-1}.

4. Results

4.1. Seismo-stratigraphic framework

Previous high-resolution single- and multi-channel Boomer profiles acquired throughout the lake (Pinson, 2009; Vardy et al., 2010) defined five main seismo-stratigraphic units (SSS I to SSS V) for the Windermere sediments. Here we use a simplified version of this framework, combining SSS I and SSS II into a single seismo-stratigraphic unit (SSS I; Fig. 3), resulting in four main seismo-stratigraphic units (SSS I to SSS IV). The multi-channel boomer data achieved good penetration, allowing the construction of an interval velocity model using common-reflection point gathers, which identifies the oldest unit, SSS I, as a strongly attenuating deposit with high acoustic interval velocities between 1750 and 3500 m s^{-1} and several separate sub-units (Pinson, 2009). Unit SSS II is the thickest deposit of the sequence, with strongly layered internal reflections infilling the underlying topography of SSS I. An often disturbed, erosive deposit with weak, chaotic internal reflections (but occasionally transparent) forms unit SSS III. A draped deposit, SSS IV, which shows some low amplitude internal reflections, can be consistently identified throughout the lake and forms the youngest seismo-stratigraphic unit.

The same four main seismo-stratigraphic units can be identified in the parametric sub-bottom profiler data (Table 2). Irregular and scattering high amplitude reflections form the basal reflector of unit SSS II with no further penetration into unit SSS I or structural detail of the underlying deposit resolvable. In the central part of the study area, where the water depth is greatest and where the depocentre is located, the sediment cover was too thick to continuously map that boundary. The overlying younger unit, SSS II, forms an up to 15 m thick infilling package of parallel, continuous reflections of variable amplitude and thickness. Individual, traceable reflections become wider at greater water depths, and, in places, are observed to be cut by shallow normal faulting. We also identified SSS III as a mainly reflection free or transparent unit that occasionally scours into older strata. The youngest seismo-stratigraphic unit, SSS IV, is a draped deposit of uniform thickness (c. 3.5 m), with some low amplitude, continuous internal reflections.

Based on reflector morphologies and internal architecture, we further subdivide SSS III into three separate facies (F IIIa through IIIc; Fig. 4 and Table 2). The oldest facies, F IIIa, is a 50 to 60 cm thick uniform layer with low amplitude internal reflections, traceable throughout the deeper parts of the lake basin. Facies F IIIb varies in thickness between less than one and a few metres, thins towards the basin centre and is often located close to break of slopes. This facies occasionally scours into older strata and usually demonstrates a transparent seismic characteristic. In places, F IIIb exhibits stacked packages, divided by high amplitude reflections, but without interbedding of other facies. F IIIc is an up to 1 m thick package of layered high and low amplitude reflections, similar to the seismic characteristic of unit SSS II. If F IIIb is present, F IIIc can be observed mostly above, but locally also below these deposits.

Furthermore, we also subdivide SSS IV into two separate sub-units (SSS IVa and IVb; Fig. 4 and Table 2). SSS IVa is an up to 4 m thick uniform deposit with some low amplitude, but continuous internal reflections. SSS IVb is a reflection free upper layer of 0 to 40 cm thickness, mostly recognizable in the deeper basin and thinning out at water depths of less than 20 m.

Within SSS IVa occasionally appear locally confined and scattering high amplitude reflections, with blanking of underlying strata.

4.2. Correlation with core stratigraphy

Several short cores of 5 – 6 m length have previously been collected and analysed in both lake basins (Pennington, 1943, 1977; Smith, 1959; Mackereth, 1971; Coope et al., 1977). The main seismo-stratigraphic units SSS I through IV can be correlated against these core stratigraphies at multiple intersections throughout the lake (Fig. 4 and Table 2; Pinson, 2009; Vardy et al, 2010). The closest to our study area, Core M (Fig. 2) in the South Basin, is described by Mackereth (1971).

We correlate (Figs. 4 and 5):

- The coarsely layered seismo-stratigraphic unit SSS II with the lower part of Core M (Fig. 4). Annual varves, up to 2 cm thick, are indicative of extremely high deposition rates after the LGM and ice retreat, when sedimentation in Windermere was dominated by inorganic glacial outwash (Pennington, 1943; Coope et al., 1977).
- The uniform facies F IIIa with the distinct organic detritus silt layer of about 30 cm thickness deposited during the Windermere Interstadial (Mackereth, 1971; Coope et al., 1977).
- The usually transparent facies F IIIb with the 60 cm thick deposit of highly disturbed and disoriented material above the upper boundary of the glacial fines. In other cores, similar deposits are shown to comprise Younger Dryas age material (Pennington, 1943, 1977).
- The layered facies F IIIc with the thin layer of about 50 cm of organic-poor laminated clay (some 400 paired varves of glacial fine outwash deposits) of Younger Dryas age (Pennington, 1947; Mackereth, 1971).
- The layered sub-unit SSS IVa with organic-rich Holocene deposits, when sedimentation rates were in the range of 0.2 to 0.6 mm yr^{-1} (Chiverrell, 2006).
- The reflection free sub-unit SSS IVb with recently deposited organic ooze.

5. Mass movement deposits

Interpretation of the data set has revealed seventeen individual mass movement deposits (E-I through E-VXII), which were mapped between seismic profiles. Two mass movement deposits were emplaced within the Holocene sediments of SSS IV (Figs. 6 and 7). All other events were emplaced within the Younger Dryas sediments and identified as F IIIb, but in places scour into older strata.

The relative timing of emplacement for each event (E-I = oldest, E-XVII = youngest) has been determined based on the relative position of the bounding reflections within the seismic sections. For two events no temporal relationship could be defined, because they are spatially isolated (E-I, E-II), while some events are interpreted as being emplaced at similar times within the relative time scale (E-III + E-IV, E-VII + E-VIII, E-X + E-XI). Two representative seismic sections that intersect each other (Figs. 6 and 7) show the slope on the western side of the lake, several stacked mass movement deposits of Younger Dryas age within the central lake basin, and the two overlapping mass movement deposits within SSS IV. Fig. 8 summarizes the reflector geometries and defines the temporal relationship for all identified events. Based on the deposit morphologies and the internal structure we discuss the classification of the mass movement deposits in section 5.2.

5.1 Reflector geometries

We recognized two different styles of reflector geometries for the identified mass movement deposits in the study area (Fig. 9), which separate the Younger Dryas from the Holocene events. The majority of the Younger Dryas mass movement deposits show an almost transparent internal seismic characteristic. The lower boundary is sometimes irregular (e.g. E-VIII, E-XII; Figs. 7 and 9), but often shows a sheet-like, non-erosive characteristic (e.g. E-IV, E-XI; Fig. 7). Upper boundaries vary between slightly irregular to regular morphologies (Figs. 6, 7 and 9). E-I is the only event with evidence for thrust features, while some other events show frontal ramp features (e.g. E-VIII; Fig. 9). Occasionally we recognized step-ups and step-downs in the proximal parts of the larger events (e.g. E-I, E-VIII; Fig. 9).

The two Holocene events exhibit a highly irregular upper boundary. The modern lakebed still shows a distinct relief, even though the deposits are now draped by younger Holocene sediments. The very high amplitude, lower boundary is less irregular, but shows signs of erosion into older strata (Figs. 6, 7 and 9). The two Holocene deposits have a generally reflection-free internal architecture. Occasionally, high amplitude diffraction hyperbolas appear within these deposits.

5.2 Deposit morphologies

The Younger Dryas mass movement deposits often exhibit lobed planiform shapes and even circular shapes can be recognized where material movement is unimpeded (e.g. E-VI, E-VIII, E-XIII; Fig. 10), but become irregular when confined by features in the pathway of emplacement. Such features are palaeo-bathymetric highs (e.g. E-XV), basin borders (e.g. E-I, E-XIV) or pre-existing mass movement deposits (e.g. E-XIII). In addition, some unconfined deposits exhibit a highly irregular shape (e.g. E-XII, E-XIV), indicative of a high mobility and fluid-like deposition, which is controlled by minor palaeo-lakebed relief. For example, E-XIV flows from an underlying morphological high in both directions (Fig. 10).

Both Holocene events have a lobed shape and material spreads out unidirectionally from the foot of the slope, thinning distally. E-XVI exhibits individual finger-like features at distal parts of deposition, which are not so apparent in the gridded surfaces, while E-XVII has a surface with blocks of relatively undisturbed material. These blocks are visible in the seismic sections (Figs. 9C and 9D).

From the interpreted seismic sections we extracted upper and lower boundaries for all mass movement events. Data were gridded and values for area, volume and thickness of deposits were calculated (Table 3). We also measured the length of deposition, but due to uncertainties related to the position relative to the failure zone, we could not calculate accurate run-out values. We estimated the slope angles and basal dip angles for most of the events, using the apparent knick-point in the cross-sectional shape of the mass movement events (Table 3, Fig. 11). Histograms showed widely distributed values and did not allow a clustering of the data set with confidence, other than clearly separating the Younger Dryas and Holocene events. The Younger Dryas events usually show shallower slope angles (i.e. < 8°), shallower basal dip angles (i.e. < 1°), greater length of deposition (i.e., a higher mobility) and less thick deposits. The statistical analysis of Moernaut and De Batist (2011) has shown a wide distribution of slope angles for frontally emergent slides, between 0° and 21°, and basal slope angles in toe regions were in the range of -0.2° to 1.6° (negative values denote upslope transport). This is in good agreement with our data set (e.g. E-III with $\alpha_s = 4.7°$, $\alpha_b = 0.3°$ and E-VI with $\alpha_s = 6.8°$, $\alpha_b = 0.1°$; see also Table 3).

We analysed the ratio between volume and depositional area. Moernaut and De Batist (2011) found strong correlations for both emergent ($V = 0.0744A^{1.241}$, $R^2 = 0.939$) and confined slides ($V = 0.0727A^{1.330}$, $R^2 = 0.942$) with very good fitness values to power functions. We found a similar strong correlation, but the power functions for our emergent slides are different ($V = 0.209A^{1.1605}$, $R^2 = 0.9365$ for the Younger Dryas events and $V = 0.2504A^{1.1503}$, $R^2 = 0.8693$ for all events, including the Holocene ones). The number of events in our study is not very high and the dimensional range of the events in our data set is smaller, but the lateral and vertical resolution should give well constrained dimensional values. Furthermore, the significant decrease of fit for the power functions when Holocene events are included demonstrates the obviously different behaviour of the mass movements in these sediments at similar dimensional scales. The Holocene mass movement deposits are more localized, and remain thicker than the Younger Dryas mass movement deposits. The higher mobility of the Younger Dryas mass movements is most likely related to different properties (e.g., cohesiveness) of the deposited sediments.

6. Discussion

6.1. Pre-Younger Dryas structure

Faults and scarps have been identified and mapped within SSS II (Figs. 6, 9 and 12). The general fault trend is NNW – SSE, parallel to the lake shores. However, some scarps and one fault have an East – West orientation (Fig. 12), which are probably related to underlying moraine ridges cross-cutting the lake basin (Pinson, 2009). The bathymetry also exhibits vertical steps of several metres at these two locations. The majority of faults are normal, down-throwing towards the centre of the lake basin, indicative of general downslope transport rather than basement tectonics. The identified scarps are better preserved at shallower depths than close to the main depositional centre, where subsequent failures have eroded the older scarps and failure zones. Alternatively, some of the mapped faulted blocks could be the result of uneven topography too steep for deposition, and therefore causing the impression of vertically translated blocks.

Fluid escape features, characterized by narrow chimney like structures widening with depth (from c. 5 m on top to c. 20 m on the bottom), disrupt the sediments around the failure zones. Typically, seismic reflection amplitudes decrease within and below the chimneys (Fig. 6). When mapped in planar view the fluid escape features form distinct elongated and parallel zones in the central basin and show a North East – South West trend (Fig. 12), although there is also a scattered distribution of smaller features aligned close to the major break of slope at the western side of the lake basin. Some of these features, which disrupt the sediments, exhibit high amplitude diffraction hyperbolas. The fluid escape structures ascend until they are trapped beneath the Holocene mass movement deposits (Figs. 6 and 7), explaining the high basal reflection amplitudes.

Chapron et al. (2004) demonstrated how fluid escape features in a French lake could be linked to the development of fractures and synsedimentary faults, eventually forming the head scarp of a large mass movement. The distinct chimneys observed in Windermere terminate below the Holocene deposits, i.e. no deformation of reflections occurs above. This suggests either an early development, which stopped before the Holocene deposition occurred or very recent features, which did not have time to ascend further. Fluid escape features are commonly associated with the dewatering of porous sediments in facies assemblages. Fluid escape features are also often linked to ground shaking due to seismogenic activity (Chapron et al., 2004; Moernaut et al., 2009). We link these features to a period of increased seismic activity after the deposition of the glacio-lacustrine infill, but before the Holocene period, probably caused by isostatic adjustment. Such adjustment may also have reactivated the inferred basement fault, running along the axis of the lake, which is inferred to have the same trend and location as the linear fluid escape features (Figs. 1 and 12).

6.2. Time frame for mass movements

We correlated the thin facies of F IIIa against the organic detritus silt layer in the core, which is interpreted as Windermere Interstadial deposits, dated to 13.4 ± 0.4 ka ^{14}C BP (Mackereth, 1971). Facies F IIIc was correlated against the organic-poor glacial fines in the core, which are interpreted as resulting from deposition during the Younger Dryas cooling event (10.13 ± 0.35 ka ^{14}C BP; Mackereth; 1971). These ages are bulk ^{14}C ages, which do not provide a precise age control on the transition from the Interstadial to the Younger Dryas.

All mass movement deposits (facies F IIIb) that fill the basin of the study area are deposited above F IIIa, with the exception of localised scouring into older strata (e.g. E-I). In most cases, facies F IIIc can be observed above the most recent mass movement within the stack of events. Occasionally, F IIIc can be observed below a mass movement event (e.g. E-XII). This places the majority of the identified mass movement events within the Younger Dryas period. The large number of events for a relatively short time frame (i.e. 15 over a period of 1000 to 1200 years) suggests a rapid or catastrophic mode of deposition. The nature of possible triggering mechanisms is discussed further in Section 6.5.

While not directly sampled in existing core data, ages for the two Holocene events can be estimated based on their vertical position within the seismic unit and using an approximate sedimentation rate for Windermere during the Holocene (Figs. 6, 7 and 9). The upper boundary for these two deposits is very complex and therefore it is not possible to simply measure the thickness of the material on top. The horizon of emplacement for each event was selected as the approximate lower boundary of on-lapping deposits. Seismic sections from our data set show on-lapping Holocene sediments down to a depth of 125 cm for E-XVI and 70 cm for E-XVII. Chiverrell (2006) determined Holocene sediment accumulation rates for Windermere based on radiometric data, palaeomagnetic data and pollen marker horizons, finding a fairly constant value of 0.35 mm yr^{-1} during this period. With the ^{14}C age of 10,130 ± 350 ka BP at a depth of 290 cm in the core from the study site (Mackereth, 1971) we calculated a local value of 0.29 mm yr^{-1} ^{14}C. This relates to an approximate ^{14}C age of 2,400 years for the youngest event E-XVII, and 4,400 years for E-XVI.

Although these age values are only estimates (being based on uncalibrated early ^{14}C dates, sediment thicknesses, and local variations in accumulation rate) they raise two factors when relating the Younger Dryas and Holocene events. Firstly, the estimated ages for the Holocene mass movements are too old for an anthropogenic triggering source. Secondly, the significant time lag between the rapidly deposited mass movements during the Younger Dryas and the two Holocene mass movements suggest a different trigger or process for their emplacement.

6.3. Classification of mass movements

Several classification schemes for subaqueous mass movements exist. Based on cohesiveness and turbulence of flow Mulder and Cochonat (1996) suggest a distinction can be made between mass slides (cohesive) and gravity flows (non-cohesive). We have not identified distinct large scale blocks within the Younger Dryas mass movement deposits, rather we observe a typically homogeneous and reflection-free seismic character that suggests matrix-supported motion. This, together with the absence of distinct large blocks, would place these events, following Mulder and Cochonat (1996), as gravity flows, with a sub-classification of mass flows and further sub-classification as debris flows. However, mass movements are able to evolve between types during deposition (Mulder and Alexander, 2001), and characterisation by seismic data alone is not always sufficient for a classification, particularly in lacustrine environments where the deposit morphologies are commonly affected by limited accommodation space (Tripsanas et al., 2008).

A more general classification based on the frontal emplacement style of sub-marine mass movements has been proposed by Frey-Martinez et al. (2006). According to this, all the Younger Dryas events can be classified as ‘frontally emergent slides’, which ramp up from their basal shear surface and translate in an unconfined way over the palaeo-lakebed (Figs. 6, 7 and 9). The apparent thrust features of E-I would be indicative of a ‘frontally confined slide’, but the features are located close to the basin slope and not in a clear toe region which therefore differs from a typical frontally confined morphology (Schnellmann et al., 2005; Frey-Martinez et al., 2006).

The two Holocene events exhibit a more irregular boundary morphology, indicative of a higher degree of material cohesiveness compared to the Younger Dryas events. The Holocene events are not sampled by cores and we can only broadly classify them as gravity flows (mass flows), deposited in a frontally emergent mode.

6.4. Distribution of events

Using the temporal relationship between all mass movement events, a series of three-dimensional models with all events, key horizons and inferred flow directions was produced (Fig. 10). Generally, the direction of flow is controlled by the underlying morphology. We inferred the direction of flow from the basal slope angle, the general shape and cross-sectional profile of the individual events, identified toe regions and the position of the deposit relative to existing scarps at adjacent slopes. The direction of flow for E-I and E-II are of low confidence because major parts are not covered by the sub-bottom profiler data set. The point of origin for E-I (i.e. the adjacent slope) needs a large accommodation space to source the largest volume of transported deposits (> 100,000 m^3). The position of some observed thrust features would indicate a direction of flow along a North-South axis. Scarps are present around the northern outline, but also at the north-western side of this event (Fig. 12), close to an apparent sediment pathway source from a palaeo Cunsey Beck.

The number of Younger Dryas mass movement deposits sourced from the western side of the lake is higher than from the east (9:6). However, several large Younger Dryas events are sourced from the eastern lake shore (E-V, E-VI). The estimated volume of Younger Dryas mass movement deposits sourced from the western side (> 218,300 m^3) is two times greater than from the east (c. 104,800 m^3). The two Holocene events add c. 47,300 m^3 of deposited material sourced from the western side (Table 3), and throughout the stratigraphic sequence imaged, the locus of sediment deposition is to the west, where Cunsey Beck delivers the major sediment flux into the South Basin.

Both slopes have shown evidence for scarps and normal faults with a downthrown side towards the lake basin, indicative of mass wasting and mass transport processes. Mobilized sediments of SSS II from shallow sections of the slope were deposited entirely above F IIIa within the central lake basin, except for some scouring deposits. The biggest scarp with an approximate height of 4 m is located at the western side (Figs. 7 and 9), close to the point with the highest number of identified events (Fig. 12). Up to five Younger Dryas events are stacked above each other at this location, whereas the eastern side shows a maximum of only two stacked events. Both Holocene mass movement events have left some deposits at shallower parts of the slope and although the two lobes slightly overlap, they are separated vertically by undisturbed deposits of SSS IV.

6.5. Trigger mechanism

Various trigger mechanisms for subaqueous mass movements have been postulated for lacustrine settings including: overloading of steep slopes due to rapid sedimentation; ground shaking due to seismogenic activity; regional flooding with related catastrophic river discharge; initiation of sub-aerial debris flows; lake level variations; surface wave activity; rock falls from adjacent slopes and human activities (Locat and Lee, 2005). Seismogenic activity in particular is able to trigger synchronous events in subaqueous settings (Locat et al., 2003, Schnellmann et al., 2006).

The relatively short time span of the Younger Dryas period for the triggering of the whole complex of nested mass movements suggests a catastrophic mechanism. Within the study area no location shows any background sedimentation between the individual mass movements. This could be explained by low sedimentation rates, but is in contrast to the rapid deposition of glacigenic clays (F IIIc) during the Younger Dryas. A rapid series of events or a very catastrophic single event seems to be a more likely explanation.

Vardy et. al. (2010) postulated that an increasingly warmer and wetter climate at the end of the Younger Dryas caused an increase in terrestrial sediment run-off that, together with large volumes of rapidly deposited fine-grained glacial outwash, led to an overloading of the steep lake slopes, triggering sediment failures. However, it is difficult to see how this increase in sedimentation alone can be enough to trigger so many observed events. Additionally, in our survey we observe undeformed Younger Dryas outwash material (F IIIc) overlying the deformed, mass transport deposits of F IIIb, which implies that reworking was ongoing throughout the Younger Dryas period rather than being concentrated into a single period of intense activity during climate amelioration.

Similarly, other common triggers for lacustrine mass wasting can be ruled out. Catastrophic river discharge is an unlikely trigger for the mass movement events on the eastern shore because there is no fluvial input. Rock falls are not possible in the area (particularly to the west, which is low lying), but regional flooding may have produced sub-aerial debris flows that entered the lake. However, most of the observed scarps are found in deeper water beyond the major breaks in slope, and therefore are unlikely to be formed by sub-aerial debris flows.

Surface wave action as a trigger can be excluded by calculating the wave base, which is c. 17 m for a fetch length of 3000 m, an average water depth of 30 m and constant wind speeds of 40 m s^{-1} (Sorensen, 1993). However, seismogenic activity remains a possible scenario for the triggering of the mass movements in this area. Windermere is located within the seismic forebulge zone of the BIIS (Muir-Wood, 2000) and experiences a modern uplift rate of c. 0.4 mm yr^{-1} (Main et al., 1999), which may be the source for recent local seismogenic activity (Musson, 1998; BGS, 2011).

The two Holocene mass movement events are separated in time by several thousand years from the Younger Dryas complex and are likely to have been triggered by a different process than the Younger Dryas events. No clear failure scarps are observed, although seismic sections show much thinner Holocene deposits nearer the shore (Fig. 13), while bathymetry and Holocene isopach maps indicate the removal of Holocene sediments from some parts of the upper slope (Fig. 14). The possible source area is both large enough to accommodate the volume of the two mass movement deposits, and adjacent to the expected position of Cunsey Beck based on hydrological analysis of the catchment area (Fig. 1). Although the present river position is south of this location, the flood plain shows evidence for various changes in river course, possibly driven by recent anthropogenic activity (e.g., farming practice). Another possible scenario is that the deposited material originated from a terrestrial source, such as a landslide, and would therefore not comprise lacustrine gyttja.

The basal shear surface of E-XVII can be recognized (Fig. 13) together with a distinct block of sediment which was not transported down the entire slope (Figs. 13 and 14). A block of undisturbed material suggests a mass wasting of existing slope sediments. However, the surface depression and source area of E-XVII appears to continue towards the shore, which suggests a terrestrial influence for this event. A flood event is a likely scenario for the triggering of this mass movement, mobilising unstable organic rich sediments, fluvially deposited directly at the mouth of Cunsey Beck.

7. Conclusions

The interpretation of a high-resolution parametric sub-bottom profiler data set allowed the identification of 17 individual mass movement deposits in a lacustrine environment. The high density of the data allowed detailed geomorphological mapping of the individual events including determination of their temporal relationship. We also identified post-depositional features within the sedimentary succession, such as fluid escape structures and rotational faulting. We reconstructed a depositional history for the stratigraphic units identified in the seismic sections. Based on this seismo-stratigraphic framework, and on the distribution and interaction of the mass movement events with previous deposits, we related 15 of the mass movement events to the Younger Dryas and two of the events to the Holocene period. We conclude that:

- At the end of the Younger Dryas, climatic changes to warmer and wetter conditions would have made subaqueous slopes unstable. Similarly, larger sediment discharge rates during ice retreat would result in the rapid deposition of poorly consolidated material in the lake, effectively preconditioning sediment deposited on the steeper lake slopes for failure. Seismic activity, related to isostatic rebound, is a possible triggering mechanism for individual events.
- For the two Holocene events, which are temporally unrelated, the spatial relationship between their origins and the predicted catchment input suggests a fluvial trigger, possibly relating to flood events.

Acknowledgements

The authors are grateful to the Freshwater Biological Association (FBA) and the Centre for Ecology and Hydrology (CEH) for providing *R/V The John Lund* and facilities at Windermere. We thank Innomar Technologie GmbH for providing equipment and technical support. Furthermore, we thank Ben James for skippering the John Lund, John Davis for technical support and Martin Wilson for providing lake level data. We are grateful for the comments of two anonymous reviewers, and to Doug Masson for discussions.

References

Ballantyne, C.K., Stone, J.O., Fifield, L.K., 2009. Glaciation and deglaciation of the SW Lake District, England. implications of cosmogenic ^{36}Cl exposure dating: Proceedings of the Geologists' Association 120, 139–144.

Baster, I., Girardclos, S., Pugin, A., Wildi, W., 2003. High-resolution seismic stratigraphy of an Holocene lacustrine delta in western Lake Geneva (Switzerland). Eclogae Geologicae Helvetiae 96, 11–20.

BGS, 2011. "Ambleside Earthquake 12 September 1988", British Geological Survey [online], available at http://www.earthquakes.bgs.ac.uk/macroseismics/ambleside_macro.htm, accessed 25/08/2011

Chapron, E., Van Rensbergen, P., De Batists, M., Beck, C., Henriet, J.P., 2004. Fluid-escape features as a precursor of a large sublacustrine sediment slide in Lake Le Bourget, NW Alps, France. Terra Nova 16, 305–311.

Chiverrell, R.C., 2006. Past and future perspectives upon landscape instability in Cumbria, northwest England. Regional Environmental Change 6, 101–114.

Chiverrell, R.C., Thomas, G.S.P., 2010. Extent and timing of the Last Glacial Maximum (LGM) in Britain and Ireland: a review. Journal of Quaternary Science 25, 535–549.

Clark, C.D., Hughes, A.L.C., Greenwood, S.L., Jordan, C., Sejrup, H.P., 2010. Pattern and timing of retreat of the last British-Irish Ice Sheet. Quaternary Science Reviews, In Press.

Coope, G., Pennington, W., Mitchell, G., West, R., Morgan, A., Peacock, J., 1977. Fossil coleopteran assemblages as sensitive indicators of climatic changes during the Devensian (Last) Cold Stage [and Discussion]. Philosophical Transactions of the Royal Society of London. Series B. Biological Sciences 280, 313–340.

Frey-Martinez, J., Cartwright, J., James, D., 2006. Frontally confined versus frontally emergent submarine landslides: a 3D seismic characterization. Marine and Petroleum Geology 23, 585–604.

Haflidason, H., Sejrup, H.P., Nygard, A., Mienert, J., Bryn, P., Lien, R., Forsberg, C.F., Berg, K., Masson, D., 2004. The Storegga Slide: architecture, geometry and slide development. Marine Geology 213, 201–234.

Hühnerbach, V., Masson, D.G., 2004. Landslides in the North Atlantic and its adjacent seas: an analysis of their morphology, setting and behavior. Marine Geology 213, 343–362.

Lawrence, D.J.D., Webb, B.C., Young, B., White, D.E., 1986. The geology of the late Ordovician and Silurian rocks (Windermere Group) in the area around Kentmere and Crook. Report of the British Geological Survey 18, No. 5.

Locat, J., Martin, F., Locat, P. Leroueil, S., Levesque, C., Konrad, J.M., Urgeles, R., Canals, M., Duchesne, M.J., 2003. Submarine Mass movements in the Upper Saguenay Fjord, (Quebec, Canada), triggered by the 1663 earthquake. In: Locat, J., Mienert, J. (Eds.), Submarine Mass Movements and their Consequences. Kluwer, 2003, 497–507.

Locat, J., Lee, H.J., 2005. Subaqueous debris flows. In: Jacob, M., Hungr, O. (Eds.), Debris-flow Hazards and Related Phenomena. Springer, Berlin, Heidelberg, 2005, 203–245.

Lowe, J.J., Rasmussen, S.O., Björck, S., Hoek, W.Z., Steffensen, J.P., Walker, M.J.C., Yu, Z.C., the INTIMATE group, 2008. Synchronisation of palaeoenvironmental events in the North Atlantic region during the Last Termination: a revised protocol recommended by the INTIMATE group. Quaternary Science Reviews 27, 6–17.

Mackereth, F., 1971. On the variation in direction of the horizontal component of remnant magnetisation in lake sediments. Earth and Planetary Science Letters 12, 332–338.

Main, I., Irving, D., Musson, R., Reading, A., 1999. Constraints on the frequency-magnitude relation and maximum magnitudes in the UK from observed seismicity and glacio-isostatic recovery rates. Geophysical Journal International 137, 535–550.

Masson, D.G., Harbitz, C.B., Wynn, R.B., Pedersen, G., Løvholt, F., 2006. Submarine landslides: processes, triggers and hazard prediction. Philosophical Transactions of the Royal Society A: Mathematical, Physical and Engineering Sciences 364, 2009–2039.

McDougall, D., 2001. The geomorphological impact of Loch Lomond (Younger Dryas) stadial plateau icefields in the central Lake District, northwest England. Journal of Quaternary Science 16 (6), 531–543.

Millward, D., Johnson, E.W., Beddoe-Stephens, B., Young, B., Kneller, B.C., Lee, M.K., Fortey, N.J., 2000. British Geological Survey: Geology of the Ambleside district. Memoir for 1:50 000 Geological Sheet 38 (England and Wales), London, The Stationary Office.

Moernaut, J., De Batist, M., Heirman, K., Van Daele, M., Pino, M., Brummer, R., Urrutia, R., 2009. Fluidization of buried mass-wasting deposits in lake sediments and its relevance for paleoseismology: results from a reflection seismic study of lakes Villarrica and Calafquén (South-Central Chile). Sedimentary Geology 213 (3–4), 121–135.

Moernaut, J., De Batist, M., 2011. Frontal emplacement and mobility of sublacustrine landslides: Results from morphometric and seismostratigraphic analysis. Marine Geology 285, 29–45.

Muir-Wood, R., 2000. Deglaciation Seismotectonics: a principal influence on intraplate seismogenesis at high latitudes. Quaternary Science Reviews 19, 1399–1411.

Mulder, T., Cochonat, P., 1996. Classification of offshore mass movements. Journal of Sedimentary Research 66 (1), 43–57.

Mulder, T., Alexander, J., 2001. The physical character of subaqueous sedimentary density flows and their deposits. Sedimentology 48 (2), 269–299.

Mullins, H.T., Halfman, J.D., 2001. High-Resolution Seismic Reflection Evidence for Middle Holocene Environmental Change, Owasco Lake, New York. Quaternary Research 55, 322–331.

Musson, R.M.W., 1998. The Barrow-in-Furness Earthquake of 15 February 1865: Liquefaction from a Very Small Magnitude Event. Pure and Applied Geophysics 152, 733–745.

Pennington, W., 1943. Lake sediments: the bottom deposits of the north basin of Windermere, with special reference to the Diatom Succession. New Phytologist 42 (1), 1–27.

Pennington, W., 1947. Studies of the Post-Glacial History of British Vegetation. VII. Lake Sediments: Pollen Diagrams from the Bottom Deposits of the North Basin of Windermere. Philosophical Transactions of the Royal Society of London. Series B. Biological Sciences 233, 137–175.

Pennington, W., 1977. The Late Devensian flora and vegetation of Britain. Philosophical Transactions of the Royal Society of London. Series B. Biological Sciences 280, 247–271.

Pinson, L.J.W., 2009. Derivation of Acoustic and Physical Properties from High-Resolution Seismic Reflection Data. PhD Thesis, National Oceanography Centre Southampton, University of Southampton, UK.

Schnellmann, M., Anselmetti, F., Giardini, D., McKenzie, J., Ward, S., 2002. Prehistoric earthquake history revealed by lacustrine slump deposits. Geology 30 (12), 1131–1134.

Schnellmann, M., Anselmetti, F.S., Giardini, D., McKenzie, J.A., 2005. Mass movement induced fold-and-thrust belt structures in unconsolidated sediments in Lake Lucerne (Switzerland). Sedimentology 52 (2), 271–289.

Schnellmann, M., Anselmetti, F.S., Giardini, D., McKenzie, J.A., 2006. 15,000 Years of mass-movement history in Lake Lucerne: Implications for seismic and tsunami hazards. Eclogae Geologicae Helvetiae 99, 409–428.

Scholz, C.A., 2001. Applications of seismic sequence stratigraphy in lacustrine basins. In: Last, W.M. and Smol, J.P. (Ed.), Tracking Environmental Change Using Lake Sediments, Volume 1. Kluwer Academic Publishers, Dordrecht, The Netherlands, 7–22.

Shen, Z., Bloemendal, J., Mauz, B., Chiverrell, R.C., Dearing, J.A., Lang, A., Qingsong, L., 2008. Holocene environmental reconstruction of sediment-source linkages at Crummock Water, English Lake District, based on magnetic measurements. The Holocene 18, 129–140.

Sissons, J., 1980. The Loch Lomond Advance in the Lake District, northern England. Transactions of the Royal Society of Edinburgh: Earth Sciences 71, 13–27.

Sorensen, R.M., 1993. Basic wave mechanics: for coastal and ocean engineers. Wiley-Interscience, New York.

Smith, A., 1959. Structures in the stratified late-glacial clays of Windermere, England. Journal of Sedimentary Petrology 29, 447–453.

Telfer, M.W., Wilson, P., Lord, T.C., Vincent, P.J., 2009. New constraints on the age of the last ice sheet glaciation in NW England using optically stimulated luminescence dating. Journal of Quaternary Science 24 (8), 906–915.

Todd, B.J., Lewis, C.F.M., Anderson, T.W., 2008. Quaternary features beneath Lake Simcoe, Ontario, Canada: drumlins, tunnel channels, and records of proglacial to postglacial closed and overflowing lakes. Journal of Palaeolimnology 39, 361–380.

Tripsanas, E.K., Piper, D.J.W., Jenner, K.A., Bryant, W.R., 2008. Submarine mass-transport facies: new perspectives on flow processes from cores on the eastern North American margin. Sedimentology 55 (1), 97–136.

Vardy, M.E., Pinson, L.J.W., Bull, J.M., Dix, J.K., Henstock, T.J., Davis, J.W., Gutowski, M., 2010. 3D seismic imaging of buried Younger Dryas mass movement flows: Lake Windermere, UK. Geomorphology 118, 176–187.

Waldmann, N., Anselmatti, F.S., Ariztegui, D., Austin, J.A., Pirouz, M., Moy, C.M., Dunbar, R., 2011. Holocene mass-wasting events in Lago Fagnano, Tierra del Fuego (54°S): implications for paleoseismicity of the Magallanes-Fagnano transform fault. Basin Research 23, 171–190.

Wunderlich, J., Wendt, G., Müller, S., 2005. High-resolution echo-sounding and detection of embedded archaeological objects with nonlinear sub-bottom profilers. Marine Geophysical Researches 26, 123–133.

Table 1

Overview of acquisition parameters for the parametric sub-bottom profiler.

Parameter	Setting for site survey	Modified setting for regional lines
Primary source level	> 236 dB re 1µPa @ 1 m	-
Secondary source level	> 200 dB re 1µPa @ 1 m	-
Primary centre frequency	100 kHz	-
Secondary frequency	12 kHz	-
Beam angle	3.8° @ -3 dB	-
Transmitter pulse length	83 µs	167 µs
Recording range	72 ms TWT (~53 m)	85 ms TWT (~64 m)
Sampling interval	10 µs	-
Ping rate	approx. 10 s^{-1}	approx. 7 s^{-1}

Table 2

Summary of stratigraphic framework with Seismic-Stratigraphic Sequence (SSS), seismo-stratigraphic facies as determined from parametric sub-bottom profiler system, core data (after Mackereth, 1971) and our stratigraphic interpretation.

SSS	Facies	Parametric SBP	Core Data with ^{14}C ages (Mackereth, 1971)	Interpretation
IVb		0 – 40 cm reflection free layer, easily penetrated by 100 kHz profiler	30 – 40cm aqueous and soft sediments, not recoverable without disturbance, organic ooze	Recently deposited organic ooze
IVa		0.5 m (shallow regions) to 4.0 m (deeper water), uniform unit with low amplitude internal reflections, occasionally appearance of biogenic gas which causes acoustical blanking of underlying strata	250 -260 cm post-glacial organic sediments, 10-15% organic carbon on dry weight, 80% interstitial water, 0,19g/ml solids 0 – 10130 ± 350 BP	Holocene deposits (Gyttja)
III	F IIIc	Up to 1 m laminated high amplitude reflections, usually visible above and sometimes below facies IIIb, but occasionally not present due to reworking	40 – 50 cm finely laminated clay, some 400 paired varves, c. 55% interstitial water, c. 1,0g/ml solids, organic free 10130 ± 350 BP – 13.400 ± 350 BP	Younger Dryas deposits
	F IIIb	< 1m up to a few metres thick, usually transparent unit, occasionally scouring into older strata, otherwise low amplitude basal reflection, resting above unit IIIa in lake basin and above unit II at some shallower slopes	50 – 60 cm slump deposits, distorted and disoriented material, angular displacement not dated	Mass movement deposits
	F IIIa	50 – 60 cm uniform layer with very low amplitude internal reflections, similar seismo-acoustic pattern as facies IVa, different appearance compared to IIIc and II, not present in shallower regions or when scoured by facies IIIb	30 cm partially organic deposits, c. 1% organic carbon dry weight, 0,78 g/ml solids bulk age of 13400 ± 350	Interstadial deposits
II		Up to 15 m laminated, high and low amplitude reflections	More than 150 cm coarsely laminated clay, paired varves up to 2 cm thick, c. 55% interstitial water, c. 1,0g/ml solids, organic free not dated	Glacio-lacustrine infill deposits
I		Upper boundary detected as irregular and scattering high amplitude reflection in shallower regions but not fully resolved in deeper parts of the lake	Not recovered (max 6 m core only)	Glacial diamict formed into a sequence of glaciogenic landforms

Table 3

Estimated quantitative properties for individual mass movement deposits, planar surface area A, volume V, maximum thickness T_m and average thickness T_a (i.e. volume divided by planar surface area, rounded to a decimetre), length of deposition L, basal dip angle α_b and adjacent slope angle α_s. Events marked (*) are under-estimates, because they are cut by the boundaries of the data set or available data are too sparse to determine the full extents. The slope angle could also not be determined with confidence for several events. Events marked (#) have no temporal relationship at all and events marked (ø) were emplaced at similar time intervals relative to younger and older events, otherwise relative age decreases from E-I to E-XVII.

Event	A [m^2]	V [m^3]	T_m [m]	T_a [m]	L [m]	α_b [°]	α_s [°]
SSS IV							
E-XVII	20300	29900	2.7	1.5	230	1.2	7.7
E-XVI	9300	17400	3.0	1.9	160	1.7	16.3
SSS III							
E-XV	12800	12400	1.8	1.0	150	0.4	7.0
E-XIV	25500	20800	1.7	0.8	240	0.6	7.0
E-XIII	20800	26500	4.0	1.3	220	0.2	2.2
E-XII	20200	24400	2.2	1.2	220	0.4	4.9
E-XI (ø)	6700	4400	1.0	0.7	100	1.2	14.9
E-X (*)(ø)	4700	3900	1.3	0.8	>110	0.9	n/a
E-IX	2400	2100	1.7	0.9	75	3.1	n/a
E-VIII (ø)	19000	18400	2.6	1.0	175	0.4	8.0
E-VII (*)(ø)	3300	4700	2.6	1.4	>60	1.8	n/a
E-VI	16400	22100	1.8	1.3	240	0.1	6.8
E-V	17900	18300	2.0	1.0	250	0.4	3.6
E-IV (ø)	10100	7000	1.1	0.7	150	0.3	n/a
E-III (ø)	8900	7800	1.5	0.9	125	0.3	4.7
E-II (*)(#)	>32800	>42600	3.8	1.3	>230	0.4	3.7
E-I (*)(#)	>29400	>107700	6.8	3.7	>250	2.2	13.4

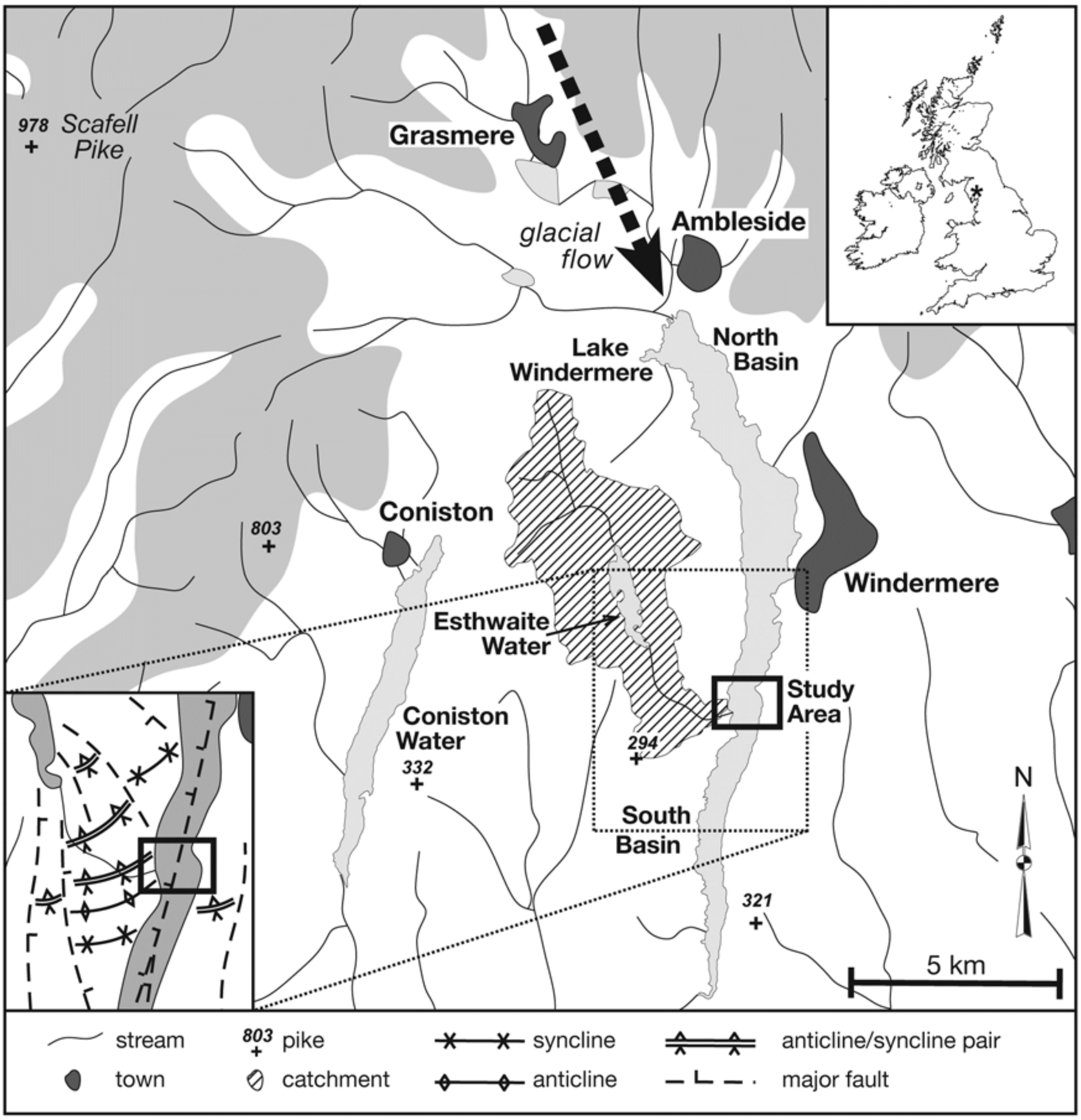

Fig. 1. Regional map of southern Lake District (upper right inset shows location in the UK). Highlands (grey, pike heights in metres), streams and lakes are indicated. Location of study area is marked with black rectangle, arrow indicates general ice flow direction and the main catchment for the South Basin is shown (diagonal hatching). Lower left inset shows bedrock geology around study area with major faults (ticks indicate downthrown side), anticlines and synclines.

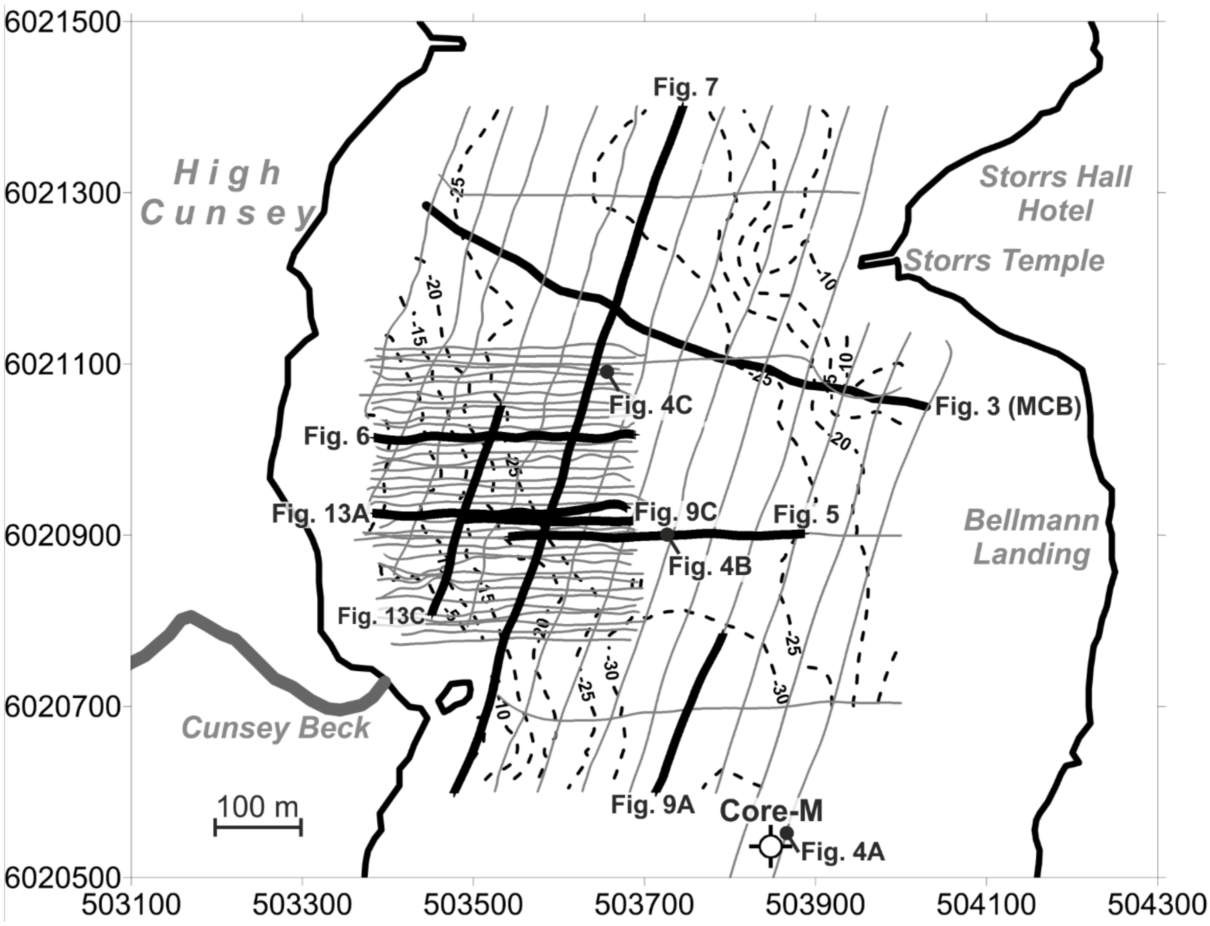

Fig. 2. Detailed map of survey area. The positions of sub-bottom profiles (grey), multi-channel boomer profile (MCB), location of core (Core-M) and paper figures (black bold lines) are indicated. The positions of the lakeshore and Cunsey Beck are shown.

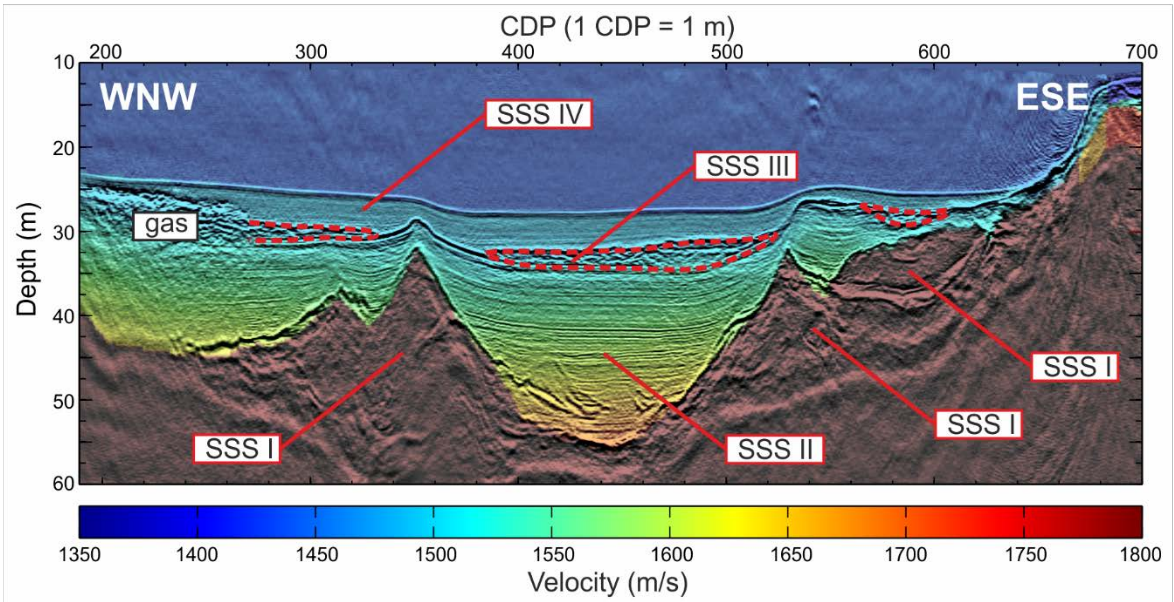

Fig. 3. Depth migrated multi-channel Boomer line (MCB Line) coloured by P-wave interval velocity and labelled with main seismo-stratigraphic units (after Pinson, 2009). Mass movement deposits are bounded by red dotted lines. Profile location shown in Fig. 2. Vertical exaggeration = 5:1.

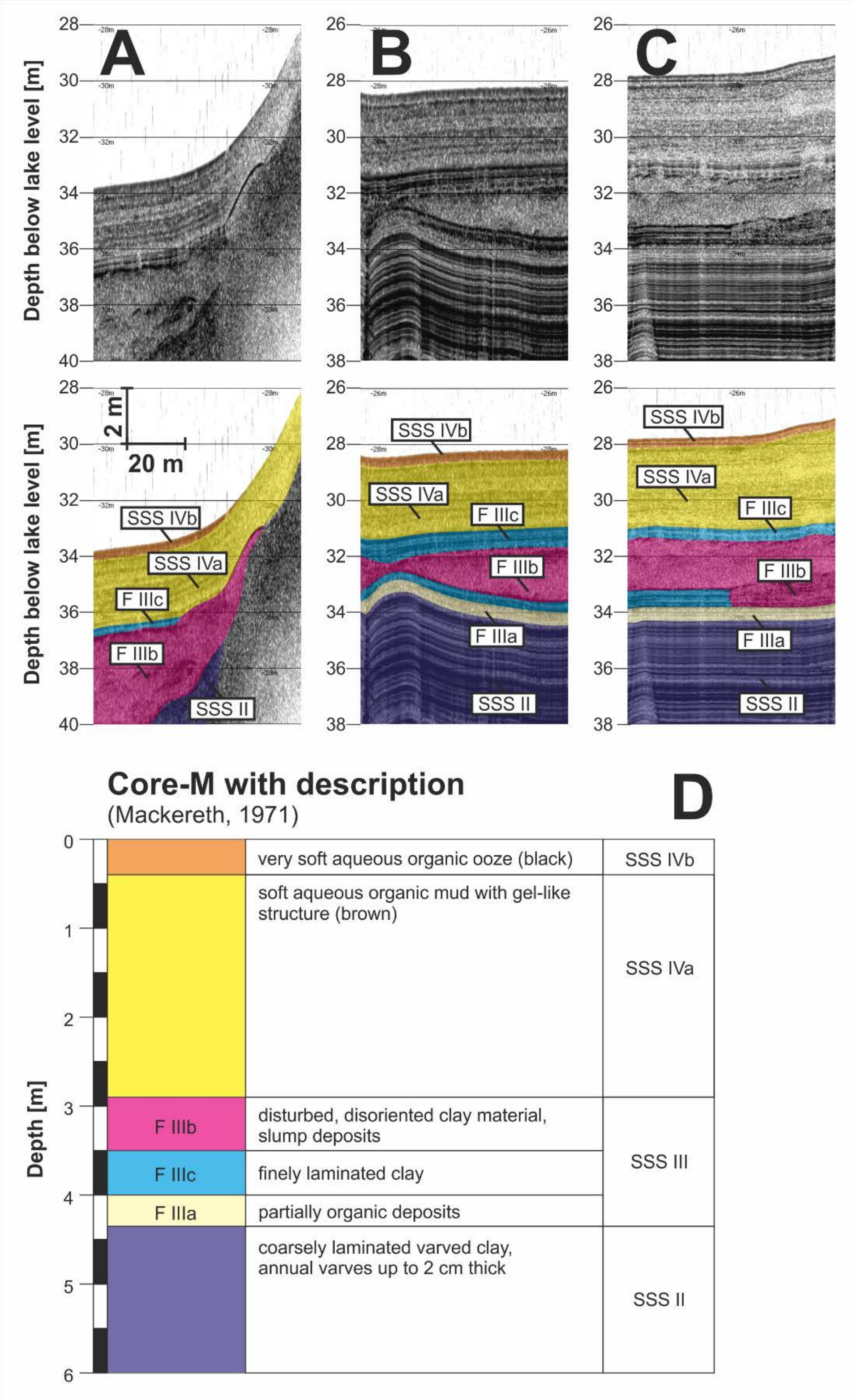

Fig. 4. Short seismic sections with and without interpretation: (A) close to the core location; (B) from the study area and c. 300 m North of the core location; (C) from the study area and c. 500 m North of the core location. Core-M (D) was described by Mackereth (1971). Note the comparable seismo-acoustic characteristic of the thin crème coloured (at 4.0 to 4.3 m in the core) and the thick yellow coloured (at 0.4 to 2.9 m in the core) reflection package. See Fig. 2 for profile locations. Vertical exaggeration = 10:1.

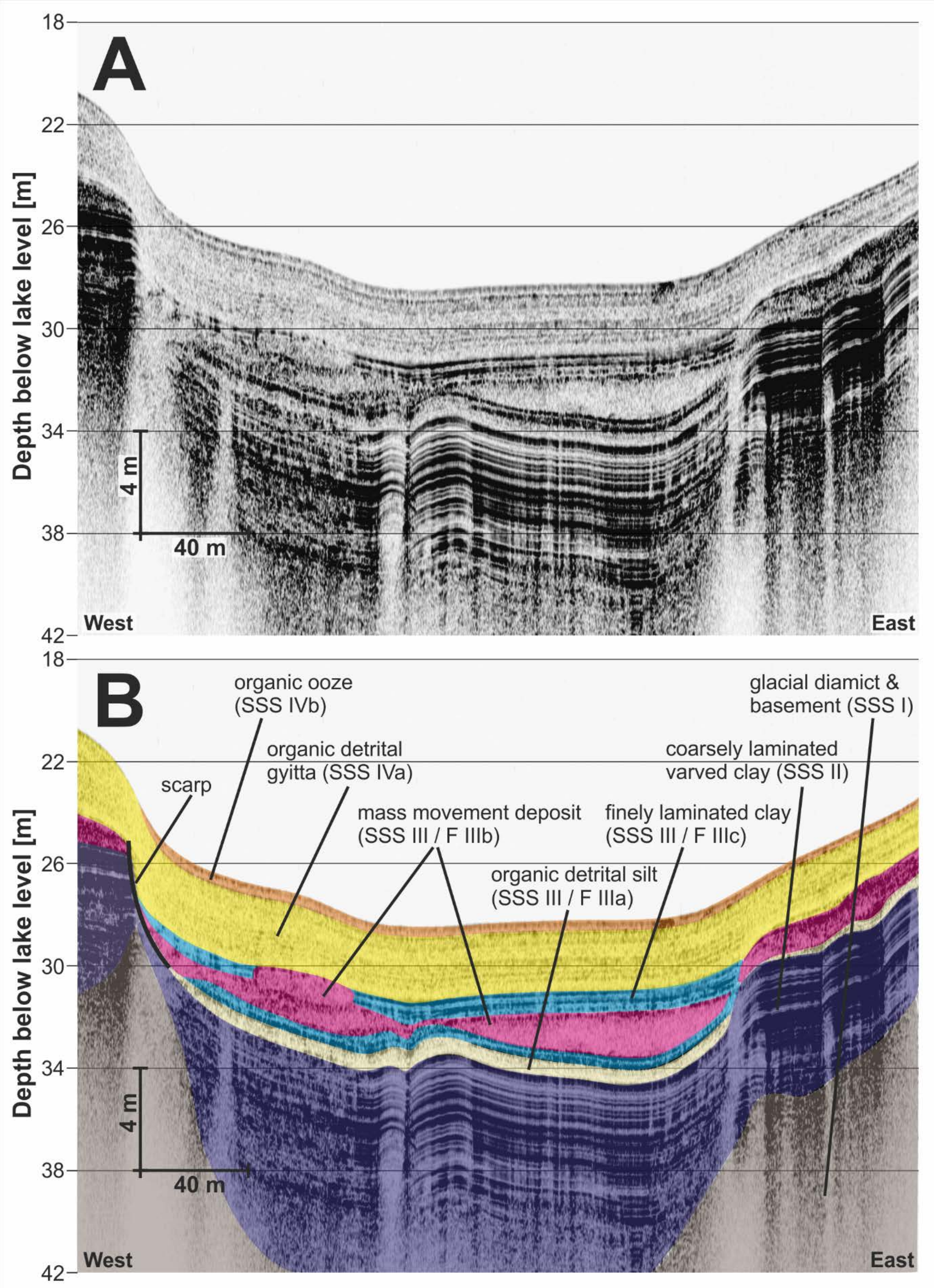

Fig. 5. Parametric sub-bottom profiler seismic section: (A) uninterpreted; (B) interpreted section with seismo-stratigraphic units and facies based on the core and seismic interpretation description in Table 2. See Fig. 2 for profile location. Vertical exaggeration = 10:1.

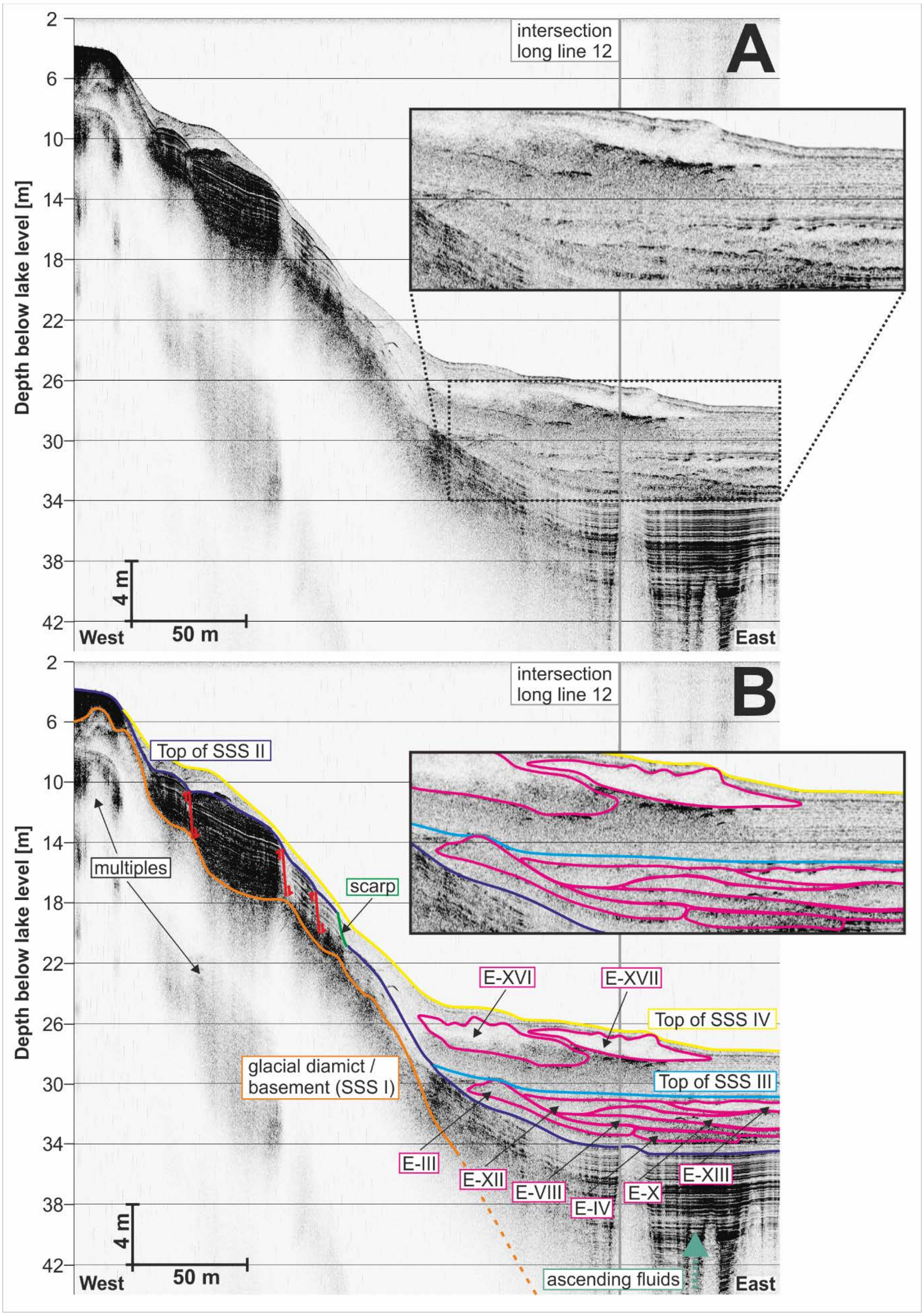

765
766 **Fig. 6.** Parametric sub-bottom profiler seismic section crossing the lake: (A) uninterpreted; (B) interpreted section, imaging both
767 Holocene events and several Younger Dryas events. See Fig. 2 for profile location. Vertical exaggeration = 6:1.
768

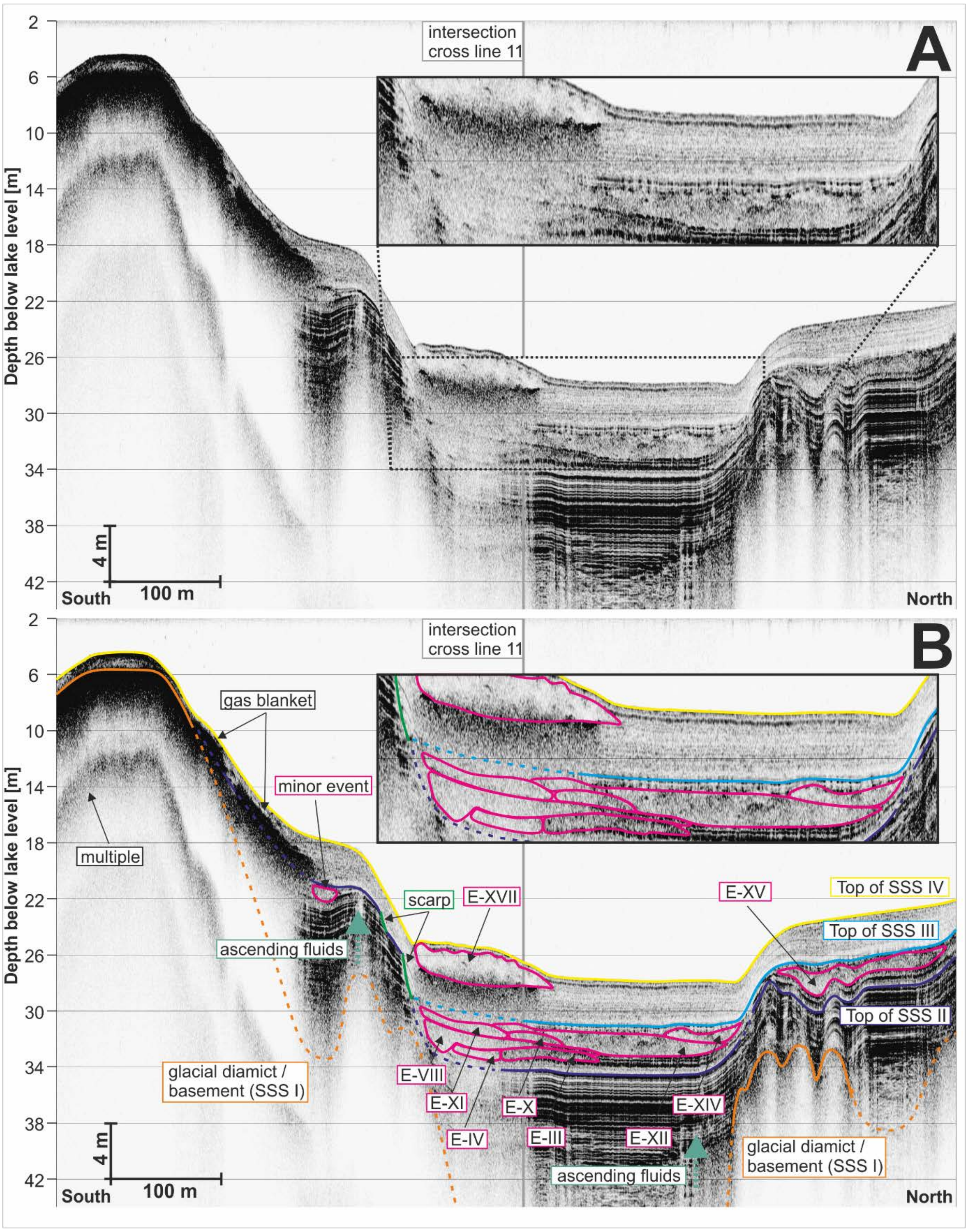

Fig. 7. Parametric sub-bottom profiler seismic section running along the lake axis: (A) uninterpreted; (B) interpreted section with two marked scarps in the lower slope deposits and indication of ascending fluids within the postglacial deposits. See Fig. 2 for profile location. Vertical exaggeration = 12:1.

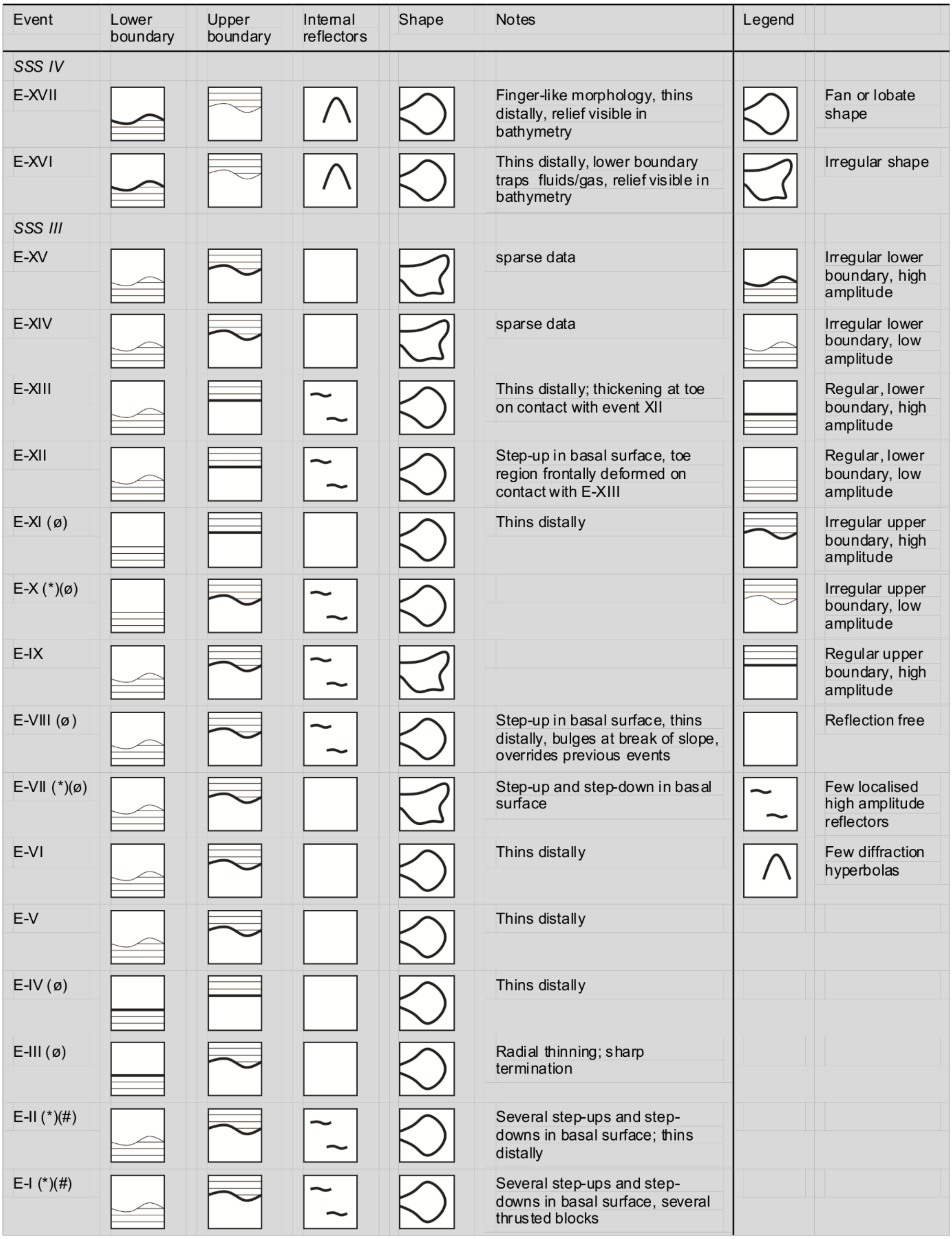

Fig. 8. Description of reflector geometries and properties for individual mass movement deposits. A legend summarises symbols used to describe lower boundary, upper boundary, internal reflections and deposit shape. Events marked (*) are cut by the boundaries of the data set or data is sparse; Events marked (#) have no temporal constraints. Events marked (ø) were emplaced at similar time intervals. In general, event relative age decreases from E-I to E-XVII.

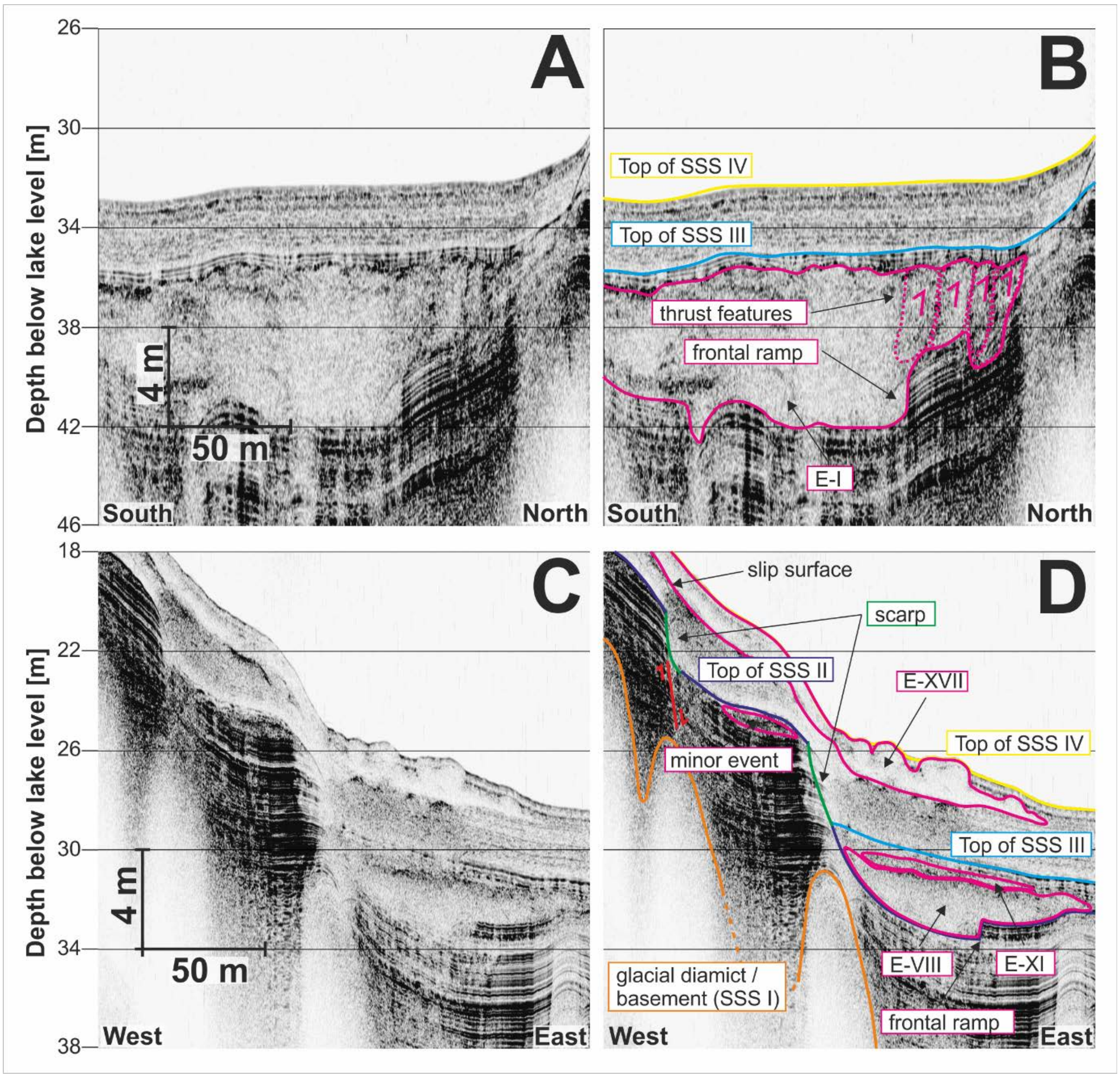

Fig. 9. Parametric sub-bottom profiler seismic sections illustrating different styles of reflector geometries: (A) uninterpreted section; (B) interpreted section with thick erosive mass movement deposit E-I with ramp and thrust features; (C) uninterpreted section; (D) interpreted section with highly irregular Holocene mass movement deposit E-XVII possibly with individual blocks. Note that for the upper seismic section (A, B) the direction of movement is oblique to the seismic profile. Profile locations are shown in Fig. 2. Vertical exaggeration = 10:1.

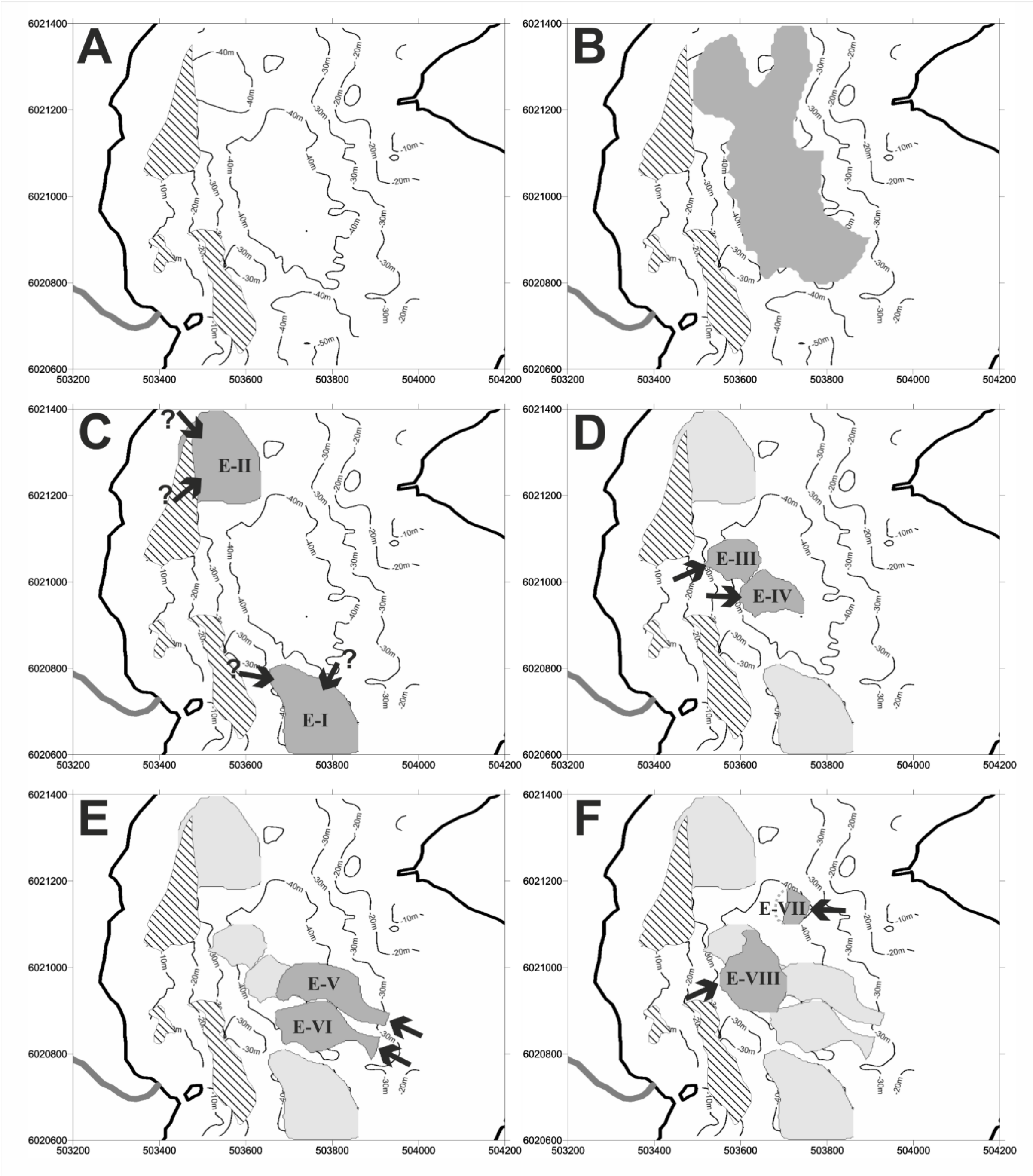

Fig. 10. The plan view geometry of all the mass movement events and relationship to key surfaces: (A) basement and ice retreat surface (top of SSS I); (B) top of interstadial layer of facies F IIIa; (C-I) individual events in temporal order as given in Fig. 8; (J) the pre-Holocene palaeo-bathymetry (bottom of SSS IV); (K) two Holocene mass movement events; (L) current lakebed, gridded from sub-bottom profiler data. Striped patches on the western lake slope are areas with shallow biogenic gas within the Holocene sediments. The lakeshore and Cunsey Beck are indicated by bold lines.

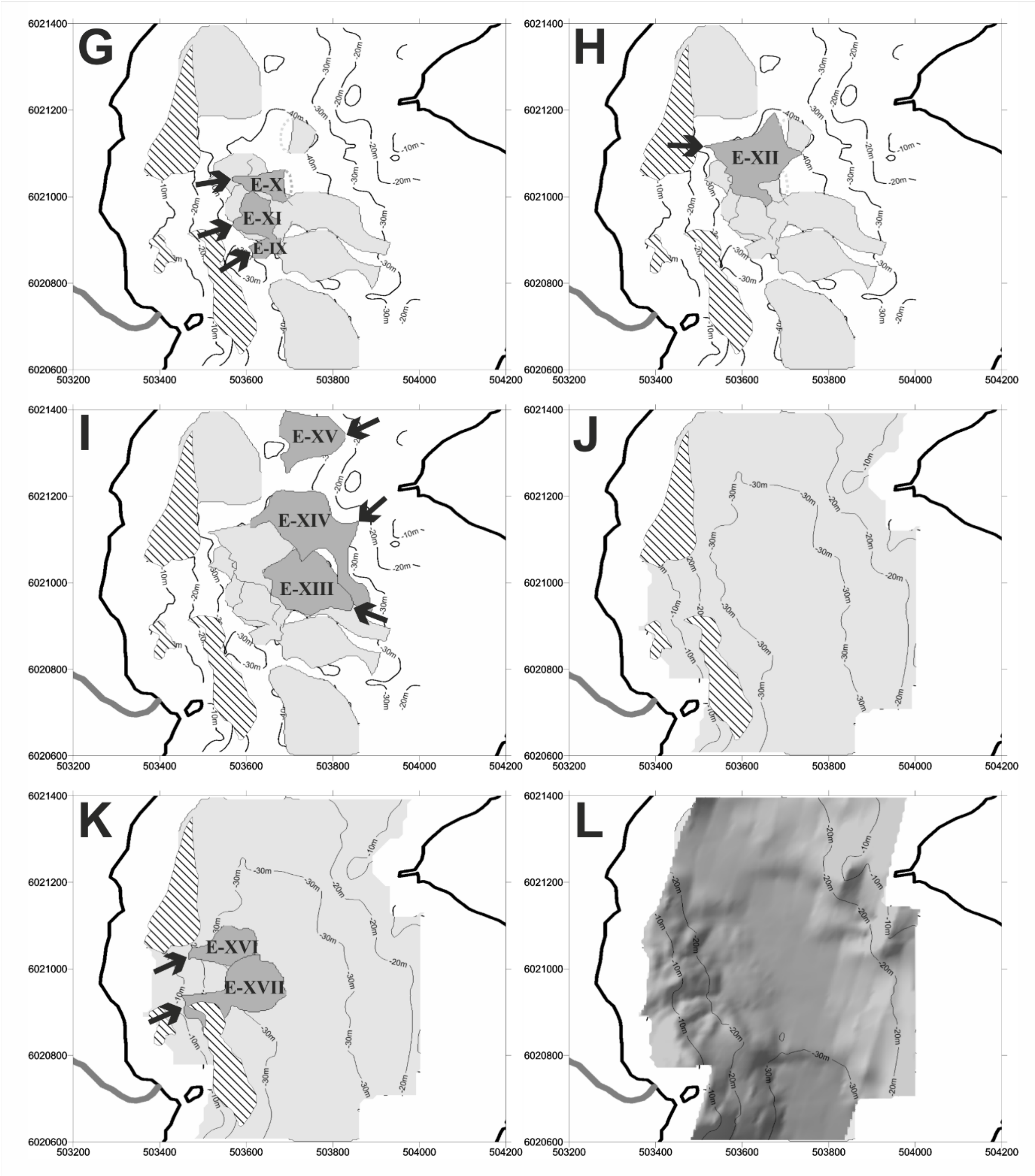

Fig. 10. The plan view geometry of all the mass movement events and relationship to key surfaces: (A) basement and ice retreat surface (top of SSS I); (B) top of interstadial layer of facies F IIIa; (C-I) individual events in temporal order as given in Fig. 8; (J) the pre-Holocene palaeo-bathymetry (bottom of SSS IV); (K) two Holocene mass movement events; (L) current lakebed, gridded from sub-bottom profiler data. Striped patches on the western lake slope are areas with shallow biogenic gas within the Holocene sediments. The lakeshore and Cunsey Beck are indicated by bold lines.

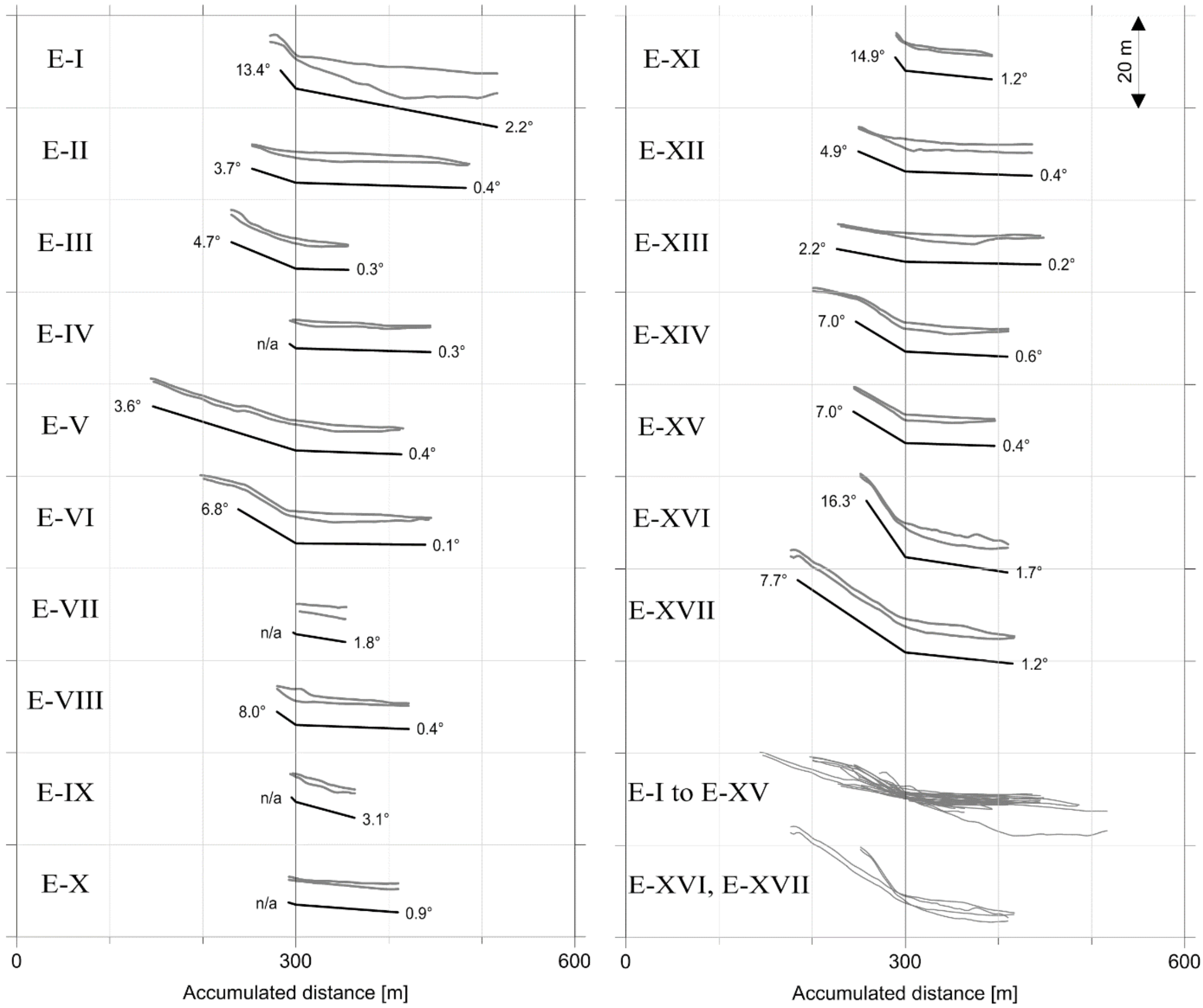

Fig. 11. Cross sectional geometry of all the mass movement deposits with slope angle α_s and basal dip angle α_b (Table 3). Lower right shows a superposition of all the Younger Dryas and Holocene event geometries to enable comparison.

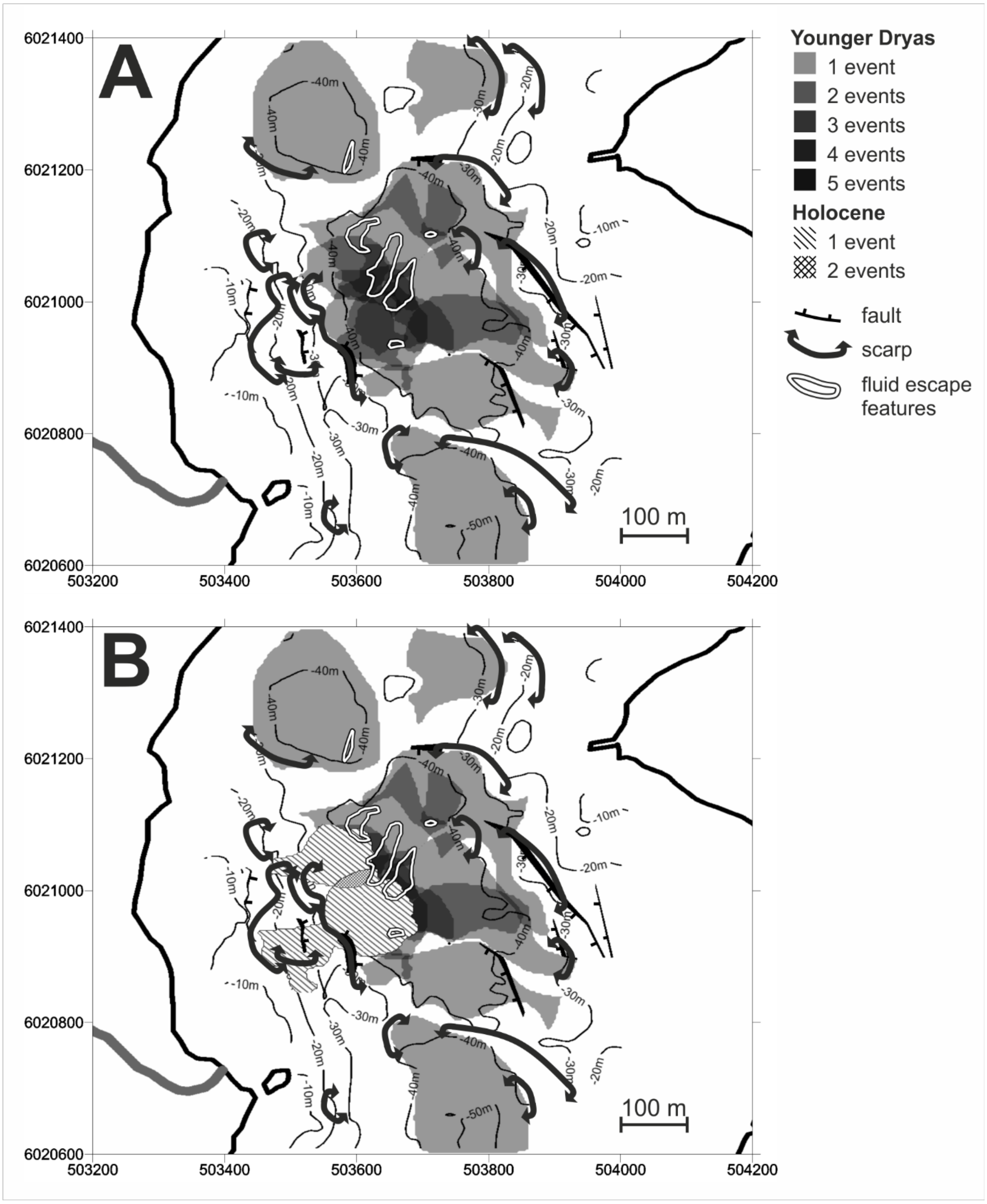

Fig. 12. Plan view map showing stacked series of mass movement events which: (A) occurred during the Younger Dryas period (grey); (B) occurred during the Holocene period (stippled). 10 m contour lines of the underlying ice retreat surface (thin black lines), faults (with tick marks on the downthrown side), scarps (with arrows towards the failure zone), and areas with discrete chimneys of ascending fluids (white polygons) are indicated. The positions of the lake shore and Cunsey Beck are shown.

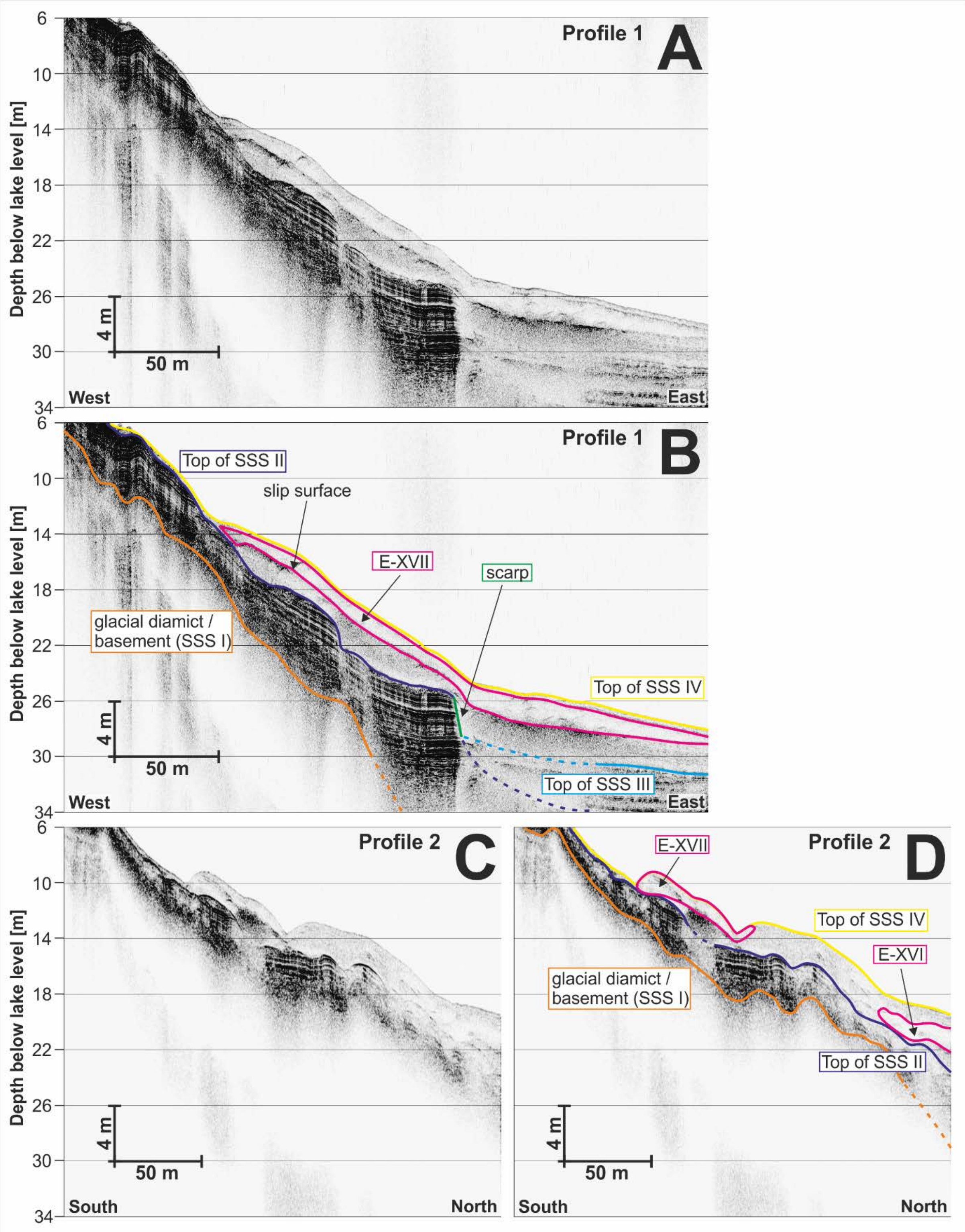

Fig. 13. Parametric sub-bottom profiler seismic sections crossing the source area of E-XVII (plan view shown in Fig. 14): (A) uninterpreted section; (B) interpreted section with a sediment slab (part of E-XVII), still resting on the slope and the related slip surface; (C) uninterpreted section; (D) interpreted section with a sediment slab (part of E-XVII), still resting on the slope and the related slip surface. Profile locations are shown in Figs. 2 and 14. Vertical exaggeration = 6:1 (A, B) and 8:1 (C, D).

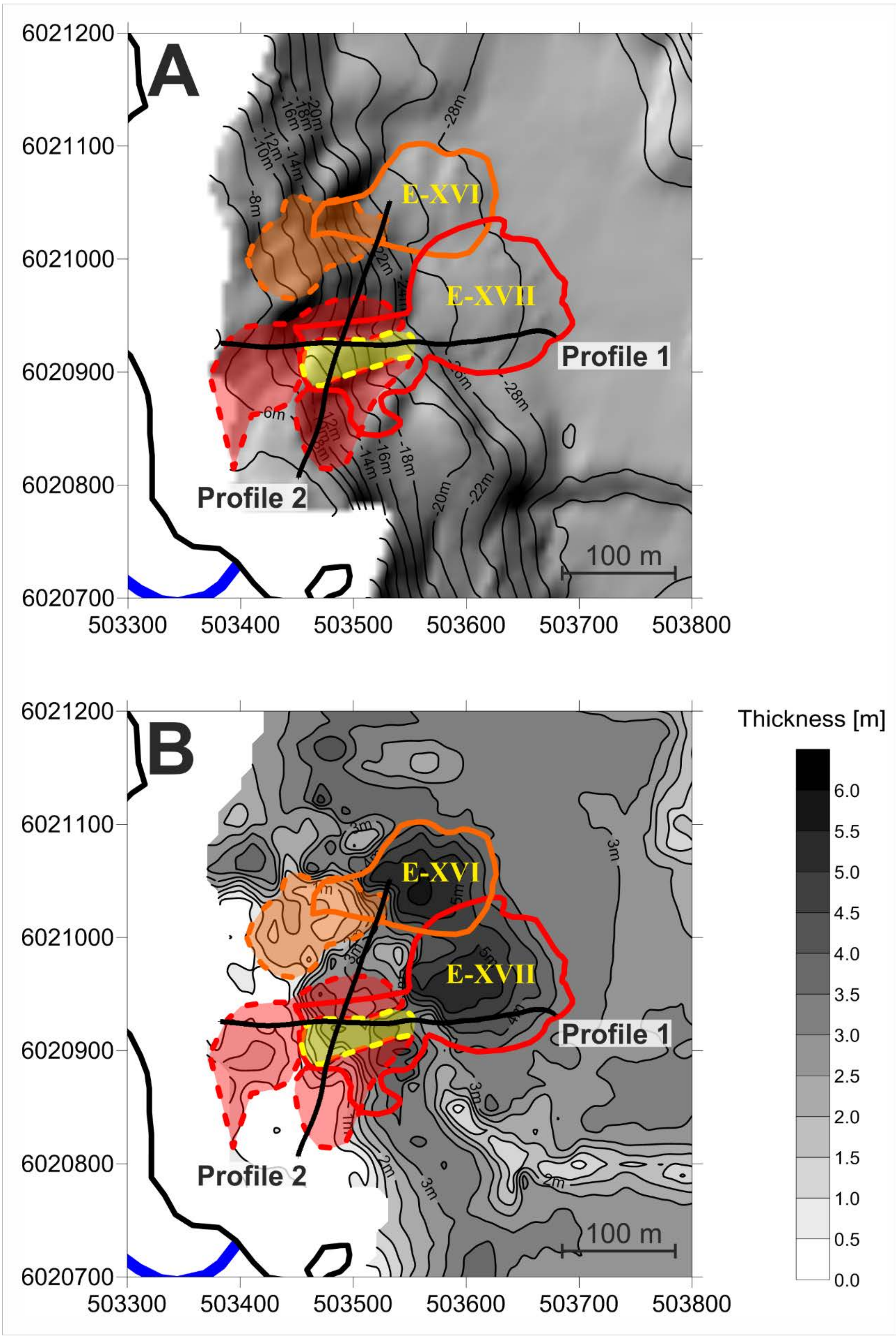

Fig. 14. (A) Shaded relief bathymetry, gridded from sub-bottom profiler data with overlay of mass movement deposits (red/orange outlines), sediment source areas (red/orange shaded), and untransported sediment slab (yellow shaded). The positions of two profiles illustrated in Fig. 13 are also shown. (B) Holocene Isopach map in m with the same overlay as for (A).